A 3-D Model for 5-HT_{1A}-Receptor Agonists Based on Stereoselective Methyl-Substituted and Conformationally Restricted Analogues of 8-Hydroxy-2-(dipropylamino)tetralin

Charlotta Mellin,[†] Jerk Vallgårda,[†] David L. Nelson,[‡] Lena Björk,[§] Hong Yu,[§] Nils-Erik Andén,[∥] Ingeborg Csöregh,[⊥] Lars-Erik Arvidsson,[†] and Uli Hacksell*[,†]

Department of Organic Pharmaceutical Chemistry, Uppsala Biomedical Centre, Uppsala University, S-751 23 Uppsala, Sweden, Department of Pharmacology and Toxicology, College of Pharmacy, University of Arizona, Tucson, Arizona 85721, Department of Medical Pharmacology, Uppsala Biomedical Centre, Uppsala University, S-751 24 Uppsala, Sweden, Department of Pharmacology, Karolinska Institutet, Box 60400, S-104 01 Stockholm, Sweden, and Department of Structural Chemistry, Arrhenius Laboratory, Stockholm University, S-106 91 Stockholm, Sweden. *Received March 2, 1990*

The enantiomers of *cis*- and *trans*-1,2,3,4,4a,5,10,10a-octahydro-9-hydroxy-1-propylbenzo[*g*]quinolines (**10** and **11**, respectively) and the enantiomers of *trans*-1,2,3,4,4a,5,6,10b-octahydro-10-hydroxy-4-propylbenzo[*f*]quinoline (**12**) have been synthesized and their stereochemical and conformational characteristics have been studied by use of X-ray crystallography and molecular mechanics (MMP2) calculations. The compounds, which are conformationally restricted analogues of the potent 5-hydroxytryptamine (5-HT) receptor agonist 8-hydroxy-2-(dipropylamino)tetralin (8-OH-DPAT; **1**) have been evaluated for central 5-HT and dopamine receptor stimulating activity by use of biochemical and behavioral tests in rats. In addition, we have evaluated the ability of these compounds and a number of previously reported analogues to displace [^{3}H]-8-OH-DPAT from 5-HT_{1A}-binding sites. The enantiomers of **12** behave as potent 5-HT_{1A}-receptor agonists, whereas the octahydrobenzo[*g*]quinoline derivatives are much less potent or inactive. In general, the affinities of the compounds correlate well with their agonist potencies. The set of compounds under study is accommodated by a novel computer-graphics-derived model for 5-HT_{1A}-receptor agonism. The model consists of a flexible pharmacophore and a partial receptor-excluded volume.

Introduction

Considerable research efforts have been devoted to drugs interacting with 5-hydroxytryptamine (5-HT; serotonin) receptors of the 5-HT_{1A} subtype[1,2] and a substantial number of analogues to the potent and selective agonist 8-hydroxy-2-(dipropylamino)tetralin (**1**; 8-OH-DPAT)[3] have been reported.[4] Nevertheless, the apparently complicated structure–activity relationships (SAR) of 5-HT_{1A}-receptor agonists containing a phenethylamine moiety have been poorly understood.[5] This may be demonstrated by the absence of a satisfactory rationale for the varying stereoselectivity of 2-aminotetralins and related serotonergic agents (Figure 1); for example, whereas **1** is weakly stereoselective,[3a,4b] several 2-aminotetralin derivatives (**2–4**; Figure 1)[4c,d,6] and phenylcyclopropylamines (**5** and **6**; Figure 1)[7] exhibit a considerable stereoselectivity when interacting with 5-HT_{1A} receptors.

The tricyclic 2-aminotetralin congeners **10–13** (Figure 1) may be considered as conformationally restricted analogues of **2–4** and **7**. The enantiomers of octahydrobenzo[*f*]quinoline derivative **13** were recently reported to be of low potency as 5-HT-receptor agonist,[4f] the 4a*R*,10b*S* enantiomer apparently being responsible for most of the activity of the racemate. In order to further explore the SAR of 5-HT_{1A}-receptor agonists related to **1**, we have now synthesized the enantiomers of octahydrobenzoquinoline derivatives **10–12**.

The molecular conformations of the crystallized hydrochloride salts of (4a*S*,10b*S*)-**12**, (4a*S*,10a*R*)-**15**, and (4a*S*,10a*S*)-**18** [the two latter being precursors to (4a*S*,10a*R*)-**10** and (4a*S*,10a*S*)-**11**, respectively] have been determined by single-crystal X-ray diffraction analysis and their absolute configurations have been deduced by measuring the anomalous dispersion effects.[8] The new compounds have been investigated pharmacologically by use of biochemical and behavioral tests in rats. In addition, we have evaluated the affinity of the enantiomers of **1–6** and **10–12** as well as that of the racemic **7–9** for [^{3}H]-8-

[†] Department of Organic Pharmaceutical Chemistry, Uppsala University.
[‡] Department of Pharmacology and Toxicology, University of Arizona.
[§] Department of Medical Pharmacology, Uppsala University.
[∥] Department of Pharmacology, Karolinska Institutet.
[⊥] Department of Structural Chemistry, Stockholm University.

(1) The 5-HT_{1A} receptor has been cloned and expressed: Fargin, A.; Raymond, J. R.; Lohse, M. J.; Kobilka, B. K.; Caron, M. G.; Lefkowitz, R. J. *Nature* **1988**, *335*, 358–360.
(2) 5-HT_{1A}-receptor agonists appear to be of clinical value as anxiolytic agents: Traber, J.; Glaser, T. *Trends Pharmacol. Sci.* **1987**, *8*, 432–437.
(3) (a) Arvidsson, L.-E.; Hacksell, U.; Nilsson, J. L. G.; Hjorth, S.; Carlsson, A.; Lindberg, P.; Sanchez, D.; Wikström, H. *J. Med. Chem.* **1981**, *24*, 921–923. (b) Arvidsson, L.-E.; Hacksell, U.; Johansson, A. M.; Nilsson, J. L. G.; Lindberg, P.; Sanchez, D.; Wikström, H.; Svensson, K.; Hjorth, S.; Carlsson, A. *J. Med. Chem.* **1984**, *27*, 45–51. (c) Hjorth, S.; Carlsson, A.; Lindberg, P.; Sanchez, D.; Wikström, H.; Arvidsson, L.-E.; Hacksell, U.; Nilsson, J. L. G. *J. Neural Transm.* **1982**, *55*, 169–188. (d) Gozlan, H.; El-Mestikawy, S.; Pichat, L.; Glowinsky, J.; Hamon, M. *Nature* **1983**, *305*, 140–142. (e) Middelmiss, D. N.; Fozard, J. R. *Eur. J. Pharmacol.* **1983**, *90*, 151–153. (f) Tricklebank, M. D.; Forler, C.; Fozard, J. R. *Eur. J. Pharmacol.* **1985**, *106*, 271–282. (g) Hoyer, D.; Engel, G.; Kalkman, H. O. *Eur. J. Pharmacol.* **1985**, *118*, 13–23. (h) Engel, G.; Göthert, M.; Hoyer, D.; Schlicker, E.; Hillenbrandt, K. *Naunyn-Schmiedeberg's Arch. Pharmacol.* **1986**, *332*, 1–7.
(4) See, for example: (a) Liu, Y.; Mellin, C.; Björk, L.; Svensson, B.; Csöregh, I.; Helander, A.; Kenne, L.; Andén, N.-E.; Hacksell, U. *J. Med. Chem.* **1989**, *32*, 2311–2318. (b) Björk, L.; Backlund Höök, B.; Nelson, D. L.; Andén, N.-E.; Hacksell, U. *J. Med. Chem.* **1989**, *32*, 779–783. (c) Mellin, C.; Björk, L.; Karlén, A.; Johansson, A. M.; Sundell, S.; Kenne, L.; Nelson, D. L.; Andén, N.-E.; Hacksell, U. *J. Med. Chem.* **1988**, *31*, 1130–1140. (d) Arvidsson, L.-E.; Johansson, A. M.; Hacksell, U.; Nilsson, J. L. G.; Svensson, K.; Hjorth, S.; Magnusson, T.; Carlsson, A.; Andersson, B.; Wikström, H. *J. Med. Chem.* **1987**, *30*, 2105–2109. (e) Mellin, C.; Liu, Y.; Hacksell, U.; Björk, L.; Andén, N.-E. *Acta Pharm. Suec.* **1987**, *24*, 153–160. (f) Wikström, H.; Andersson, B.; Elebring, T.; Jacyno, J.; Allinger, N. L.; Svensson, K.; Carlsson, A.; Sundell, S. *J. Med. Chem.* **1987**, *30*, 1567–1573. (g) Wikström, H.; Elebring, T.; Hallnemo, G.; Andersson, B.; Svensson, K.; Carlsson, A.; Rollema, H. *J. Med. Chem.* **1988**, *31*, 1080–1084. (h) Thorberg, S.-O.; Hall, H.; Åkesson, C.; Svensson, K.; Nilsson, J. L. G. *Acta Pharm. Suec.* **1987**, *24*, 169–182. (i) Cossery, J. M.; Gozlan, H.; Spampinato, U.; Perdicakis, C.; Guillaumet, G.; Pichat, L.; Hamon, M. *Eur. J. Pharmacol.* **1987**, *140*, 143–155. (j) Naiman, N.; Lyon, R.; Bullock, A.; Rydelek, L.; Titeler, M.; Glennon, R. A. *J. Med. Chem.* **1989**, *32*, 253–256. (k) Backlund Höök, B.; Yu, H.; Mezei, T.; Björk, L.; Svensson, B.; Andén, N.-E.; Hacksell, U. *Eur. J. Med. Chem.*, in press.

0022-2623/91/1834-0497$02.50/0

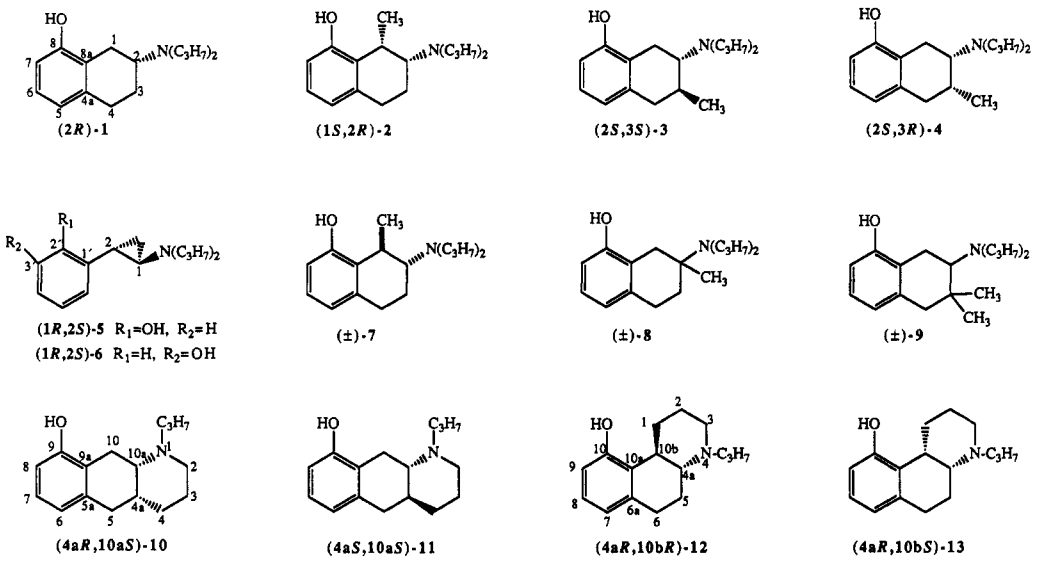

Figure 1. Structures of compounds discussed.

OH-DPAT-labeled 5-HT_{1A}-binding sites in vitro.

On the basis of molecular mechanics derived energies and geometries of potential bioactive conformations of the compounds discussed, we have developed a 3-D model which accounts for observed pharmacological activites of these compounds. The model, which may be of predictive value, consists of a flexible pharmacophore and partial 5-HT_{1A}-receptor-excluded volume.

Chemistry

Synthesis. The *N*-benzyl substituted *cis*- and *trans*-octahydrobenzo[*g*]quinoline derivatives (±)-14 and (±)-18

were prepared from 1,7-dimethoxynaphthalene by facile and stereoselective synthetic routes.[9] Racemic 14 and 18 were resolved into the enantiomers by fractional crystallization of the diastereomeric dibenzoyl- and di-*p*-toluoyltartrates, respectively. N-Debenzylation [H_2/Pd-(C)/MeOH] of the racemates and enantiomers of 14 and 18 gave the corresponding secondary amines[9] 15 and 19 (method I). The enantiomeric excess of these enantiomers was determined by GC analyses of the *O*-methylmandeloylamides to be >96% ee, respectively.

Racemic 12 has been prepared previously but the synthesis suffered from poor yields of several intermediates.[10]

Scheme I[a]

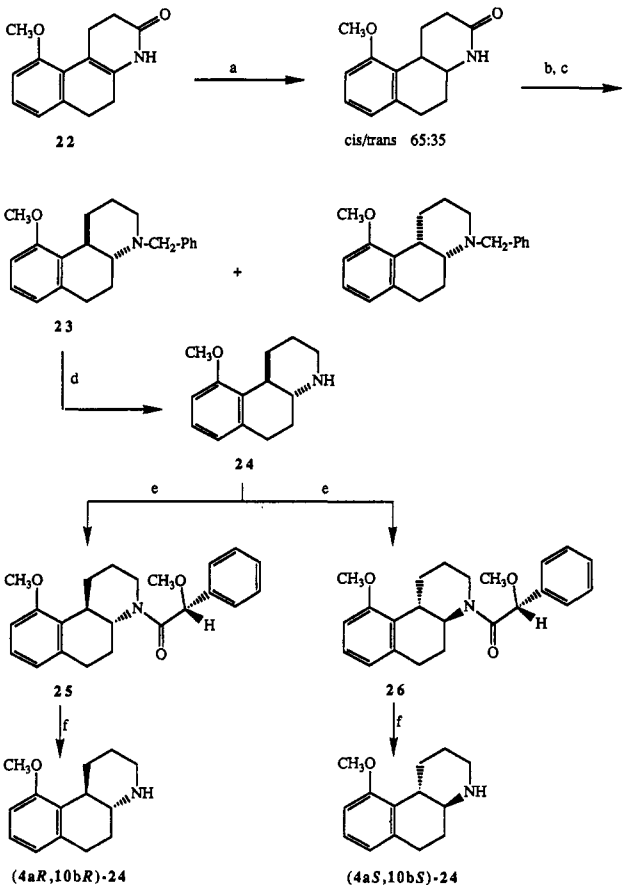

[a] Reagents: (a) $SiHEt_3$, CF_3COOH, CH_2Cl_2; (b) $LiAlH_4$, THF; (c) (i) $PhCH_2Cl$, K_2CO_3, CH_3CN, (ii) flash chromatography; (d) HCl, H_2, Pd(C), MeOH; (e) (i) (*R*)-2-OMe-2-$PhCH_2COCl$, CH_2Cl_2, 1 M NaOH, (ii) flash chromatography; (f) $LiEt_3BH$, THF.

In an attempt to improve the stereoselectivity of the synthetic sequence, we reduced the 4a,10b double bond of 1,4,5,6-tetrahydro-10-methoxybenzo[*f*]quinolin-3-(2*H*)-one (22)[10] with triethylsilane/trifluoroacetic acid, a

(5) Arvidsson, L.-E.; Karlén, A.; Norinder, U.; Sundell, S.; Kenne, L.; Hacksell, U. *J. Med. Chem.* **1988**, *31*, 212–221.
(6) For more detailed pharmacological evaluations of 2–4, see: Björk, L.; Mellin, C.; Hacksell, U.; Andén, N.-E. *Eur. J. Pharmacol.* **1987**, *143*, 55–63. Hjorth, S.; Sharp, T.; Hacksell, U. *Eur. J. Pharmacol.* **1989**, *170*, 269–274. Hjorth, S.; Sharp, T.; Liu, Y. *Naunyn Schmiedeberg's Arch. Pharmacol.* **1990**, *341*, 149–157.
(7) Arvidsson, L.-E.; Johansson, A. M.; Hacksell, U.; Nilsson, J. L. G.; Svensson, K.; Hjorth, S.; Magnusson, T.; Carlsson, A.; Lindberg, P.; Andersson, B.; Sanchez, D.; Wikström, H.; Sundell, S. *J. Med. Chem.* **1988**, *31*, 92–99.
(8) Bijvoet, J. M.; Peerdeman, A. F.; van Bommel, A. J. *Nature* **1951**, *168*, 271–272.
(9) Mellin, C.; Hacksell, U. *Tetrahedron* **1987**, *43*, 5443–5450.
(10) Wikström, H.; Sanchez, D.; Lindberg, P.; Arvidsson, L.-E.; Hacksell, U.; Johansson, A.; Nilsson, J. L. G.; Hjorth, S.; Carlsson, A. *J. Med. Chem.* **1982**, *25*, 925–931.

Table I. Physical Data of Some Octahydrobenzo[*g*]- and [*f*]quinolines

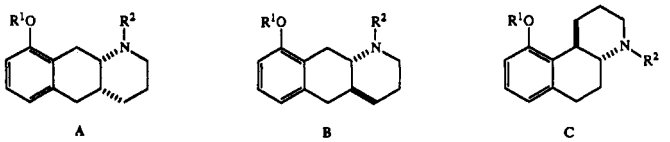

compd	general structure	R^1	R^2	prepn method[a]	yield %	mp, °C	recrystn solvents[b]	formula	$[\alpha]^{D}$,[c] deg
14	A	Me	Bz	*d*	42	100–101	A	$C_{21}H_{25}NO$	
(4a*S*,10a*R*)-14	A	Me	Bz	*a*	69	117–119	A	$C_{21}H_{25}NO$	−78.6[e]
(4a*R*,10a*S*)-14	A	Me	Bz	*a*	63	116–118	A	$C_{21}H_{25}NO$	+77.8[e]
15	A	Me	H	*d*	88	226–228	B	$C_{14}H_{19}NO{\cdot}HCl$	
(4a*S*,10a*R*)-15	A	Me	H	I	76	269–270	B	$C_{14}H_{19}NO{\cdot}HCl$	+29.5
(4a*R*,10a*S*)-15	A	Me	H	I	79	269–271	B	$C_{14}H_{19}NO{\cdot}HCl$	−30.3
(4a*S*,10a*R*)-16	A	H	H	II	64	263–265	B	$C_{18}H_{17}NO{\cdot}HCl$	+28.8
(4a*R*,10a*S*)-16	A	H	H	II	53	264–265	B	$C_{18}H_{17}NO{\cdot}HCl$	−29.8
17	A	Me	Pr	III	88	228–230	B	$C_{17}H_{25}NO{\cdot}HCl$	
(4a*S*,10a*R*)-17	A	Me	Pr	III	85	*f*	C	$C_{17}H_{25}NO{\cdot}HCl{\cdot}{}^1/_2H_2O$	−69.5
(4a*R*,10a*S*)-17	A	Me	Pr	III	92	*f*	C	$C_{17}H_{25}NO{\cdot}HCl{\cdot}{}^1/_2H_2O$	+70.0
10	A	H	Pr	II	77	*f*	B	$C_{16}H_{23}NO{\cdot}HCl{\cdot}H_2O$	
(4a*S*,10a*R*)-10	A	H	Pr	II	91	*g*	*h*	$C_{16}H_{23}NO{\cdot}HCl{\cdot}{}^1/_4H_2O$[i]	−63.1
(4a*R*-10a*S*)-10	A	H	Pr	II	85	*g*	*h*	$C_{16}H_{23}NO{\cdot}HCl$[j]	+63.3
18	B	Me	Bz	*d*	41	216–218	D	$C_{21}H_{25}NO{\cdot}HCl{\cdot}{}^1/_2H_2O$	
(4a*S*,10a*S*)-18	B	Me	Bz	*a*	58	235–237	B	$C_{21}H_{25}NO{\cdot}HCl{\cdot}{}^1/_4H_2O$	+73.8
(4a*R*,10a*R*)-18	B	Me	Bz	*a*	63	249–250	B	$C_{21}H_{25}NO{\cdot}HCl{\cdot}{}^2/_3H_2O$	−74.9
19	B	Me	H	*d*	43	265–266	D	$C_{14}H_{19}NO{\cdot}HCl$	
(4a*S*,10a*S*)-19	B	Me	H	I	81	267–269	B	$C_{14}H_{19}NO{\cdot}HCl$	+97.3
(4a*R*,10a*R*)-19	B	Me	H	I	70	267–269	B	$C_{14}H_{19}NO{\cdot}HCl$	−97.0
(4a*S*,10a*S*)-20	B	H	H	II	58	349–350	B	$C_{13}H_{17}NO{\cdot}HCl{\cdot}{}^1/_4H_2O$	+95.9
(4a*R*,10a*R*)-20	B	H	H	II	64	350–351	B	$C_{13}H_{17}NO{\cdot}HCl{\cdot}{}^1/_4H_2O$	−95.9
21	B	Me	Pr	III	80	246–247	B	$C_{17}H_{25}NO{\cdot}HCl{\cdot}{}^1/_4H_2O$	
(4a*S*,10a*S*)-21	B	Me	Pr	III	83	269–270	B	$C_{17}H_{25}NO{\cdot}HCl$	+131.5
(4a*R*,10a*R*)-21	B	Me	Pr	III	75	270–272	B	$C_{17}H_{25}NO{\cdot}HCl$	−131.6
11	B	H	Pr	II	84	280[k]	B	$C_{16}H_{23}NO{\cdot}HCl$	
(4a*S*,10a*S*)-11	B	H	Pr	II	84	295[k]	B	$C_{16}H_{23}NO{\cdot}HCl$	+133.2
(4a*R*,10a*R*)-11	B	H	Pr	II	89	295[k]	B	$C_{16}H_{23}NO{\cdot}HCl$	−132.9
24	C	Me	H	I	91	279–280[l]	E	$C_{14}H_{19}NO{\cdot}HCl$	
(4a*R*,10b*R*)-24	C	Me	H	V	66	282–284	E	$C_{14}H_{19}NO{\cdot}HCl$	+185.3
(4a*S*,10b*S*)-24	C	Me	H	V	62	282–284	E	$C_{14}H_{19}NO{\cdot}HCl$	−211.9
(4a*R*,10b*R*)-25	C	Me	COCH(OMe)Ph	IV	72	134–136	A	$C_{23}H_{27}NO_3$	+201.3
(4a*S*,10b*S*)-26	C	Me	COCH(OMe)Ph	IV	50	131–133	A	$C_{23}H_{27}NO_3$	−298.4
(4a*R*,10b*R*)-27	C	Me	Pr	III	61	248–250	E	$C_{17}H_{19}NO{\cdot}HCl{\cdot}{}^1/_4H_2O$	+183.6
(4a*S*,10b*S*)-27	C	Me	Pr	III	69	248–250	E	$C_{17}H_{19}NO{\cdot}HCl$	−185.2
(4a*R*,10b*R*)-12	C	H	Pr	II	80	238–240	B	$C_{16}H_{23}NO{\cdot}HCl{\cdot}{}^1/_4H_2O$	+177.8
(4a*S*,10b*S*)-12	C	H	Pr	II	96	238–240	B	$C_{16}H_{23}NO{\cdot}HCl{\cdot}{}^1/_4H_2O$	−180.5

[a] See the Experimental Section. [b] A, ether/light petroleum; B, MeOH/ether; C, MeCN/ether; D, EtOH; E, EtOH/ether. [c] MeOH, *c* 1.0, except where noted. [d] See ref 9. [e] $CHCl_3$, *c* 1.0. [f] This compound is very hygroscopic and no reproducable melting point was obtained. [g] Amorphous. [h] No recrystallization. [i] Anal. Calcd for $C_{16}H_{23}NO{\cdot}HCl{\cdot}{}^1/_4H_2O$: N, 4.9. Found: N, 4.3. Mass spectrum (70 eV) *m/z* 245 (M^+). Spectral data (^1H NMR, ^{13}C NMR, and IR) were in agreement with those from (±)-**10**. [j] Anal. Calcd for $C_{16}H_{23}NO{\cdot}HCl$: N, 5.0. Found: N, 4.3. Mass spectrum (70 eV), *m/z* 245 (M^+). Spectral data (^1H NMR, ^{13}C NMR, and IR) were in agreement with those from (±)-**10**. [k] Decomposition. [l] Mp 266–269 °C is reported in ref 10.

reagent reported[11] to stereospecifically reduce derivatives of 1,2,5,6-tetrahydrobenzo[*f*]quinolin-3(4*H*)-one to the corresponding *trans*-amides. However, although a variety of reaction conditions were tried, we were never able to obtain lower cis:trans ratios than 65:35. In order to be able to separate the mixture by flash chromatography we converted the diastereomeric amides to the corresponding N-benzylated amines by reduction followed by N-benzylation (Scheme I). The relative stereochemistry of the resulting diastereoisomers was initially assigned by ^1H NMR spectroscopy.[12] The assignments were subsequently confirmed by X-ray crystallography (vide infra). N-Debenzylation of the trans derivative **23** gave the *trans*-octahydrobenzo[*f*]quinoline derivative **24**. Treatment of **24** with (−)-(*R*)-*O*-methylmandeloyl chloride produced the diastereomeric amides **25** and **26**, which were separated by flash chromatography (method IV). Reduction of **25** and **26** with lithium triethylborohydride[13] afforded the resolved amines (4a*R*,10b*R*)-**24** and (4a*S*,10b*S*)-**24**, respectively (method V). It may be noted that attempts to cleave the amides **25** and **26** by use of the procedure described by Wikström et al.[14] [(a) *t*-BuOK, THF, H_2O; (b) MeLi, THF] mainly produced dihydronaphthalene derivatives due to competing elimination processes.

Reductive alkylation of the secondary amines **15** and **19** with propionaldehyde/H_2/Pd(C) (method III) afforded the

(11) Cannon, J. G.; Chang, Y.; Amoo, V. E.; Walker, K. A. *Synthesis* **1986**, 494–496.

(12) The α-hydrogens of the *N*-benzyl group in the trans compound appeared as an AB quartet centered at 3.75 ppm with a large chemical shift difference (0.61 ppm) between the A and B portions. In contrast, the corresponding hydrogens of the cis compound appeared as apparent singlets at 3.77 and 3.75 ppm. Compare Walsh, D. A., Smissman, E. E. *J. Org. Chem.* **1974**, *39*, 3705–3708.

(13) Brown, H. C.; Kim, S. C.; Krishnamurthy, S. *J. Org. Chem.* **1980**, *45*, 1–12.

(14) Wikström, H.; Sanchez, D.; Lindberg, P.; Hacksell, U.; Arvidsson, L.-E.; Johansson, A. M.; Thorberg, S.-O.; Nilsson, J. L. G.; Svensson, K.; Hjorth, S.; Clark, D.; Carlsson, A. *J. Med. Chem.* **1984**, *27*, 1030–1036.

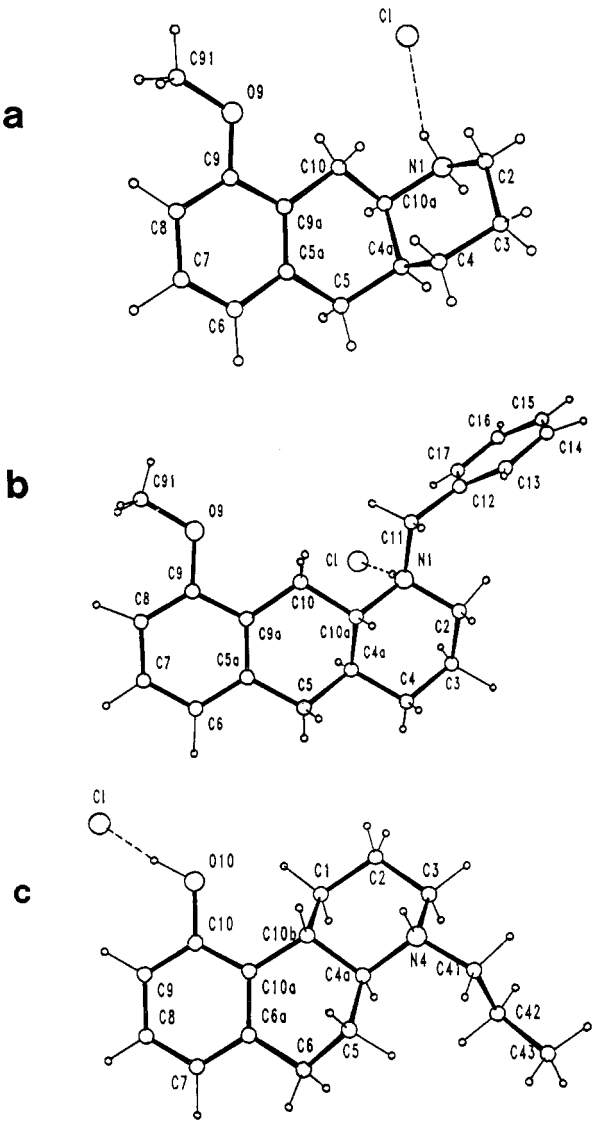

Figure 2. Perspective views showing the solid-state conformations of (a) (4a*S*,10a*R*)-**15**·HCl, (b) (4a*S*,10a*S*)-**18**·HCl, and (c) (4a*S*,10b*S*)-**12**·HCl, with atoms labeled as in the text. Solid and dashed lines represent covalent and hydrogen bonds, respectively.

N-propyl derivatives **17** and **21**, respectively. The phenols were prepared from the corresponding methoxy derivatives by treatment with aqueous 48% HBr (method II). Physical data for the new compounds are given in Table I.

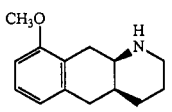

(4a*S*,10a*R*)-**15**

X-ray Crystallography. The absolute configurations of (−)-**12**·HCl, (+)-**15**·HCl, and (+)-**18**·HCl were determined according to the method of Bijvoet[8] to be 4a*S*,10b*S*, 4a*S*,10a*R*, and 4a*S*,10a*S*, respectively. The Bijvoet ratio, $X_h = 2(I_h - I_{-h})/(I_h + I_{-h})$, calculated from the received atomic positions, was compared with the observed values, based on carefully measured intensities of selected Friedel pair reflections.

For each unique *hkl* the net intensities of four equivalent reflections in the space group $P2_12_12_1$ and two equivalent reflections in the monoclinic cases were averaged for I_h and I_{-h}, respectively. The correction factors for the anomalous dispersion of the non-hydrogen atoms were taken from Cromer and Liberman.[15] The molecular structures are depicted in Figure 2.

The piperidine rings have near-chair conformation in the three structures studied. This is confirmed by the ring-puckering parameters, calculated according to Cremer and Pople[16] (supplementary material). The ideal values for a chair conformation are $\Theta = 0°$ or 180°, $q_2 = 0$ Å, and $q_3 = \pm Q$ Å.[16] However, the neighboring cyclohexene ring adopts different conformations in these compounds. In (4a*S*,10a*S*)-**18**·HCl it has an intermediate form between half-boat (or sofa) and half-chair. In (4a*S*,10b*S*)-**12**·HCl and (4a*S*,10a*R*)-**15**·HCl the cyclohexene rings adopt conformations close to a half-chair with an approximate 2-fold axis through the C(4a)–C(5) and the C(4a)–C(10a) bond, respectively.

Inspection of the calculated torsion angles[17,18] (supplementary material) shows that the nonplanar rings in (4a*S*,10b*S*)-**12**·HCl are fused in trans manner with the angular hydrogens approximately axially oriented to both rings[19] (Figure 2c). The *N*-propyl substituent has a near equatorial position. The carbon atoms of the fused benzene ring are coplanar within ±0.035 Å whereas the τ(C6a,C10a,C10,O10) and τ(C8,C9,C10,O10) torsion angles with the values 170.9(5)° and −176.0(5)°, respectively, differ from the expected 180°.

In (4a*S*,10a*R*)-**15**·HCl, both torsion angles of junction between the two nonplanar rings have the same sign, corresponding to a cis fusion, with each angular hydrogen being axial to one ring and equatorial to the other (Figure 2a). The aromatic ring is planar within ±0.027 Å with the methoxy substituent positioned close to the ring plane.

In (4a*S*,10a*S*)-**18**·HCl, the piperidine and cyclohexene rings are fused in a trans manner according to the different signs of the two torsional angles of the junction (Figure 2b). The fused benzene ring of the tricyclic moiety is coplanar within 0.014 Å and the methoxy substituent is positioned approximately in the ring plane. The *N*-benzyl substituent of the piperidine ring is equatorially oriented and its benzene ring is flat within 0.012 Å. The bond lengths and bond angles generally conform to expected values. The crystals of (4a*S*,10a*S*)-**18**·HCl contain disordered water molecules, occupying partially at least three sites.

Molecular Mechanics Calculations. In order to obtain energies and geometries of conformations of potential biological interest, we performed molecular mechanics calculations on **10**–**12**.[20] For these calculations, we used the MMP2 program developed by Allinger;[22] specifically, we used the 1980 force field,[23] to which parameters for the phenol group have been added[24] and in which updated

(15) Cromer, D. T.; Liberman, D. *J. Chem. Phys.* **1970**, *53*, 1891–1898.
(16) Cremer, D.; Pople, J. A. *J. Am. Chem. Soc.* **1975**, *97*, 1354–1367.
(17) Klyne, W.; Prelog, W. *Experientia* **1960**, *16*, 521–523.
(18) Stanford, R. H., Jr.; Waser, J. *Acta Crystallogr.* **1972**, *A28*, 213–215.
(19) Bucourt, R. *Topics Stereochem.* **1974**, *8*, 159–224.
(20) The conformational properties of **1**–**7** and **9** have been studied in detail (see refs 4c and 5) and the conformational space of the 5-hydroxyisomer of **8** has been investigated (ref 21). The conformational properties of **8** are identical with those of the regioisomer (Dr. A. M. Johansson, personal communication).
(21) Karlén, A.; Johansson, A. M.; Kenne, L.; Arvidsson, L.-E.; Hacksell, U. *J. Med. Chem.* **1986**, *29*, 917–924.
(22) Allinger, N. L. *J. Am. Chem. Soc.* **1977**, *99*, 8127–8234.
(23) Allinger, N. L.; Yuh, Y. *QCPE* **1980**, *12*, 395.

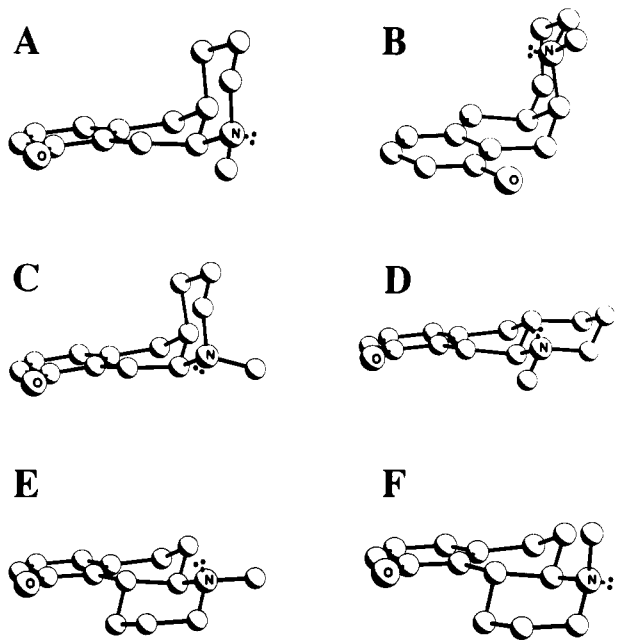

Figure 3. Low-energy conformations of (4a*R*,10a*S*)-**10** (A–C), (4a*S*,10a*S*)-**11** (D), and (4a*R*,10b*R*)-**12** (E and F). For clarity, the hydrogens have been omitted and the propyl groups have been replaced with methyl groups. Definitions of the conformations of the propyl groups and relative steric energies are given in Table II.

amine parameters[25] have been implemented. Throughout, calculations were carried out on the free bases.[26]

To identify low-energy conformations of **10**, we constructed starting geometries (using the MIMIC program)[27] by all possible combinations of tetralin ring conformations having tetralin inversion angles[4c,21] of Φ = 0°, 30°, 90°, 150°, 180°, 210°, 270°, and 330°, eight piperidine conformations symmetrically chosen along the piperidine boat-twist manifold,[28] and the two piperidine chairs, each having equatorial or axial *N*-methyl substituents. The starting geometries of **11** and **12** were obtained by adding a piperidine ring in all possible chair- and boat-forms to half chair conformations of the tetralin moiety. In all, we subjected 48, 10, and 10 starting geometries of the *N*-methyl homologues of (4a*R*,10a*S*)-**10**, (4a*S*,10a*S*)-**11**, and (4a*R*,10b*R*)-**12**, respectively, to MMP2 minimization. This procedure[29] produced the energetically favored conformers shown in Figure 3. A methyl group was added to the energy-minimized "*N*-methyl" conformations having relative steric energies below 3 kcal/mol so that three staggered "*N*-ethyl geometries" were formed from each low-energy conformation. These geometries were then minimized and the *N*-propyl conformations were finally obtained by addition of another methyl group and minimization by use of the same procedure.

Ten conformations of (4a*R*,10a*S*)-**10** with relative steric energies below 3 kcal/mol were identified (Table II). In these, the tetralin ring assumes half-chair conformations with tetralin inversion angles (Φ)[4c] around 0° or 180° and the piperidine ring adopts an almost perfect chair conformation (Figure 3). Two energetically favored ring conformations were observed: In the more stable ring conformation (A), the nitrogen assumes a pseudoequatorial disposition in relation to the tetralin moiety. In the energetically less favored conformation (B), the nitrogen is pseudoaxial. Three of the low-energy conformations of (4a*R*,10a*S*)-**10** have a pseudoaxial *N*-propyl substituent (C). However, these conformations contribute little to the

Table II. Geometrical Parameters for Low-Energy MMP2 Conformations of (4a*R*,10a*S*)-**10**, (4a*S*,10a*S*)-**11**, and (4a*R*,10b*R*)-**12**

ring conform.[a]	τ_1,[b] deg	τ_2,[c] deg	% of populn[d]	rel steric energy, kcal/mol
		(4a*R*,10a*S*)-**10**		
A	59	172	30	0
A	59	56	18	0.3
A	168	−171	17	0.4
A	168	−54	11	0.6
B	178	168	8	0.8
B	60	−177	8	0.8
B	−178	54	7	0.9
C	−60	−169	<1	2.7
C	−61	−52	<1	2.9
C	−172	168	<1	2.9
		(4a*S*,10a*S*)-**11**		
D	60	−179	38	0
D	179	169	37	0
D	−177	54	25	0.3
D	−179	−100	<1	2.7
		(4a*R*,10b*R*)-**12**		
E	−57	179	34	0
E	−176	−169	27	0.1
E	180	−55	29	0.5
E	96	−179	<1	2.5
E	−177	98	<1	2.8
E	96	61	<1	2.9
F	−175	169	6	1.1
F	−174	54	3	1.4

[a] The various ring conformations are shown in Figure 3. [b] τ_1 (For compound **10** and **11**) = τ(C10a,N,C$_\alpha$,C$_\beta$); τ_1 (for compound **12**) = τ(C4a,N,Cα,Cβ). [c] τ_2 = (N,C$_\alpha$,C$_\beta$,C$_\gamma$). [d] Based on a Boltzmann distribution at 25 °C.

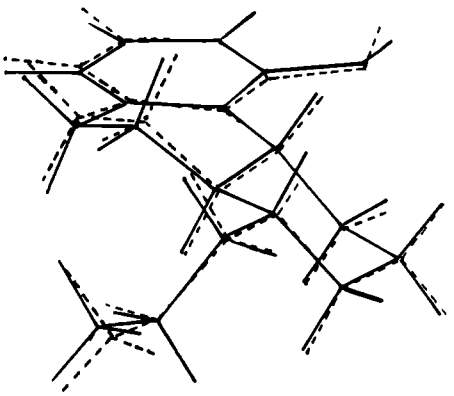

Figure 4. A computer-generated best fit of the carbon, oxygen, and nitrogen atoms of the MMP2-generated conformation of lowest energy of (4a*S*,10b*S*)-**12** (dashed lines) and the X-ray conformation (solid lines). Average distance between fitted atoms was 0.18 Å.

(24) Dodziuk, H.; von Voithenberg, H.; Allinger, N. L. *Tetrahedron* **1982**, *38*, 2811–2819.
(25) Profeta, S., Jr.; Allinger, N. L. *J. Am. Chem. Soc.* **1985**, *107*, 1907–1918.
(26) Presumably, these compounds are protonated when interacting with the receptor. However, we have observed an excellent agreement between experimentally determined conformational preferences of protonated 2-aminotetralins and calculated Boltzmann distributions of MMP2-derived conformations of the corresponding free bases.
(27) Liljefors, T. *Mol. Graphics* **1983**, *1*, 111–117.
(28) The conformational analysis was made in analogy with that of *cis*-1,2,3,4,4a,5,8,8a-octahydronaphthalene: Vanhee, P.; Tavernier, D.; Baas, J. A. M.; van der Graaf, B. *Bull. Soc. Chim. Belg.* **1981**, *90*, 697–706.
(29) Only hydroxyl group rotamers having τ(C9a,C9,O,H) ≈ 180° were considered in the calculations. Conformations having τ(C9a,C9,O,H) ≈ 0° are slightly higher in energy (0.2–0.5 kcal/mol; cf. ref 21).

overall conformational distribution of (4a*R*,10a*S*)-**10**.

Four low-energy conformations of (4a*S*,10a*S*)-**11** were identified (Table II). These differ only with respect to the conformation of the *N*-propyl substituent and may be described as fairly flat ring conformations in which the tetralin ring is a half-chair ($\Phi = 180°$) and the piperidine ring a chair (conformation D, Figure 3).

The calculations produced eight conformations of (4a*R*,10b*R*)-**12** with relative steric energies below 3 kcal/mol. In these conformations the tetralin moiety adopts a half-boat conformation ($\Phi \approx 150°$) and the piperidine moiety adopts an almost perfect chair. The most stable conformations have a pseudoequatorial N-substituent (conformation E, Figure 3). It is noteworthy that the geometry of C10 is perturbed in the eight low-energy conformations of (4a*R*,10b*R*)-**12** [τ(C6a,C10a,C10,O) = $-166.0 \pm 0.7°$ and τ(C8,C9,C10,O) = $172.8 \pm 0.4°$]. These values agree well with those found in the X-ray conformation of **12**·HCl (vide supra). In fact, the minimum-energy conformation is almost identical with the X-ray conformation (Figure 4). Apparently, the observed perturbation of C10 represents a favorable rehybridization by which the molecule relieves strain caused by the peri interaction between the oxygen substituent and a pseudoequatorial substituent at C10b.

Pharmacological Results

Biochemistry and Behavior in Vivo. It is well-known that agonists at 5-HT, dopamine (DA), and norepinephrine (NE) receptors inhibit the synthesis and utilization of the corresponding monoamine.[30] Thus, the monoamine synthesis can be used as an indicator of pre- and postsynaptic receptor activation. In the present study, the synthesis of 5-HT, DA, and NE was measured indirectly by determining the accumulation of 5-hydroxytryptophan (5-HTP) in various brain parts and of 3,4-dihydroxyphenylalanine (DOPA) in DA predominant (corpus striatum, limbic system) and NE predominant (brain stem, hemispheres) brain regions following aromatic L-amino acid decarboxylase inhibition.[31] The effects of the compounds on the monoamine synthesis in nonreserpinized rats are shown in Table III.

Stimulation of postsynaptic 5-HT and DA receptors was studied in rats in which the presynaptic monoamine stores had been depleted by reserpine pretreatment. Behavioral observations were made, particularly with regard to motility, gnawing, and sniffing (DA syndrome) and to flat body posture and foreleg movements (5-HT syndrome).[32]

The racemic cis isomer **10** (53 μmol/kg sc) did not appear to affect rat brain monoamine synthesis in nonpretreated animals and did not counteract the reserpine-induced hypomotility syndrome. Similarly, no pronounced serotonergic effects were observed after administration of (4a*R*,10a*S*)- or (4a*S*,10a*R*)-**10** (53 μmol/kg sc) or after the enantiomers of the secondary amine **16** (63 μmol/kg sc). However, the enantiomers of **10** and **16** were able to decrease the accumulation of DOPA (Table III).

The racemic trans isomer **11** (53 μmol/kg sc) did not induce any biochemical changes in nonpretreated animals. However, it produced a pronounced locomotor activity in reserpine-pretreated rats (53 μmol/kg sc). The behavioral syndrome induced by (±)-**11** included episodes of weak

Table III. Effects of Various Doses of the Enantiomers of Compound **10**, **11**, **16**, **20**, and **12** on in Vivo Accumulation of 5-HTP and DOPA and on Concentration of DA and 5-HT in the Rat Brain[a]

compd	dose, μmol/kg	5-HTP[b]				5-HT[b]		DOPA[b]				DA[b]	
		striatum	limbic	hemispheral	brain stem	striatum	limbic	striatum	limbic	hemispheral	brain stem	striatum	limbic
(4a*R*,10a*S*)-**10**	53	76.1 ± 3.8	80.6 ± 7.8*	77.9 ± 9.5	87.6 ± 5.2	118.7 ± 13.6	107.5 ± 5.2	68.3 ± 3.6**	57.7 ± 3.6**	63.0 ± 4.8**	82.3 ± 4.4*	105.3 ± 2.8	92.7 ± 4.8
(4a*S*,10a*R*)-**10**	53	81.0 ± 2.7	92.6 ± 3.7	103.9 ± 6.8	110.3 ± 4.6	100.0 ± 4.8	102.9 ± 6.1	67.2 ± 2.1**	76.9 ± 5.5**	116.0 ± 5.4	126.9 ± 8.8**	81.3 ± 4.3**	83.2 ± 3.6*
(4a*S*,10a*S*)-**11**	53	124.8 ± 16.0*	102.3 ± 8.8	113.0 ± 11.8	112.4 ± 7.2	116.9 ± 7.1	95.1 ± 4.5	91.4 ± 4.8	91.4 ± 5.3	98.8 ± 8.4	117.7 ± 6.4*	95.4 ± 3.5	87.5 ± 6.3
(4a*R*,10a*R*)-**11**	53	85.0 ± 6.9	88.0 ± 6.9	92.2 ± 3.0	91.9 ± 1.6	132.0 ± 8.4**	114.3 ± 3.5	66.1 ± 3.1**	63.8 ± 3.8**	97.5 ± 10.6	125.1 ± 6.8**	114.5 ± 3.1*	111.3 ± 3.4
(4a*S*,10a*R*)-**16**	63	102.7 ± 6.4	88.6 ± 2.6	59.7 ± 0.8**	101.7 ± 3.9	105.0 ± 7.5	92.5 ± 2.9	88.0 ± 9.5	75.3 ± 4.0**	70.4 ± 3.5**	97.7 ± 9.5	92.6 ± 5.1	73.5 ± 4.5**
(4a*R*,10a*S*)-**16**	63	108.8 ± 11.4	92.0 ± 4.5	101.4 ± 10.8	106.8 ± 8.1	100.5 ± 7.2	89.4 ± 9.2	84.0 ± 6.9	82.4 ± 6.8**	64.2 ± 5.9**	94.9 ± 4.4	92.4 ± 4.8	85.6 ± 2.6*
(4a*S*,10a*S*)-**20**	63	116.8 ± 3.9	104.6 ± 5.1	107.8 ± 7.3	115.8 ± 4.4	116.0 ± 5.3	109.6 ± 5.3	85.3 ± 3.7	85.7 ± 1.9*	85.2 ± 5.2	90.3 ± 4.6	97.4 ± 6.2	95.5 ± 7.2
(4a*R*,10a*R*)-**20**	63	96.5 ± 10.3	82.3 ± 4.5	81.9 ± 4.7	101.7 ± 8.5	100.5 ± 5.6	89.4 ± 6.9	84.2 ± 5.1	84.4 ± 4.2**	79.0 ± 6.3*	91.4 ± 7.0	92.4 ± 5.8	89.8 ± 6.3
(4a*R*,10b*R*)-**12**	3.2	34.0 ± 1.4**	50.3 ± 5.0**	50.6 ± 4.7**	59.9 ± 1.9**	128.8 ± 5.6**	144.1 ± 5.9**	99.6 ± 6.8	111.4 ± 5.0	119.0 ± 18.0	125.1 ± 6.3**	120.2 ± 4.3*	118.2 ± 4.1
	1.0	56.3 ± 1.7**	58.5 ± 7.7**	51.9 ± 5.6**	65.3 ± 6.7**	113.2 ± 7.1	119.3 ± 7.0*	116.2 ± 1.1	85.5 ± 5.7	117.0 ± 7.8	102.9 ± 9.7	129.5 ± 3.2**	95.2 ± 4.3
	0.32	69.9 ± 6.2**	85.1 ± 6.7**	70.9 ± 6.5**	76.1 ± 3.2**	107.1 ± 1.7	108.1 ± 5.0	109.4 ± 14.9	91.1 ± 3.2	111.0 ± 4.7	87.0 ± 5.8	110.6 ± 3.3	114.1 ± 3.8
(4a*S*,10b*S*)-**12**	1.0	44.7 ± 3.3**	52.3 ± 1.8**	43.0 ± 4.3**	61.1 ± 2.5**	134.9 ± 5.7**	170.1 ± 6.1**	117.6 ± 8.7	107.3 ± 3.9	140.0 ± 11.0**	133.3 ± 4.6**	115.8 ± 7.9	111.0 ± 5.8
	0.32	51.5 ± 5.5**	69.7 ± 5.0**	60.8 ± 4.4**	70.7 ± 3.8**	81.6 ± 9.0	138.1 ± 6.0**	113.6 ± 5.9	115.9 ± 6.1*	114.0 ± 18.0	110.1 ± 8.2	108.2 ± 6.2	117.8 ± 2.3*
	0.1	55.3 ± 5.8**	85.1 ± 5.1	74.7 ± 6.2**	90.8 ± 5.4	98.1 ± 4.4	126.7 ± 2.4**	109.3 ± 6.4	95.9 ± 7.5	97.0 ± 13.0	93.2 ± 5.3	123.1 ± 2.2**	124.5 ± 6.7**

[a] Nonreserpinized animals were injected with test drugs sc 60 min and NSD 1015 (287 μmol/kg sc) 30 min before death. [b] The values are percent of control, mean ± SEM (n = 15 and 4–6 in the control and experimental groups, respectively). Control means only NSD 1015 (287 μmol/kg sc) 30 min before death. Control levels for compound **10**, **11**, **16**, and **20**: (ng DOPA/g tissue) striatal 1092 ± 53.1, limbic 442 ± 13.7, hemispheral 81 ± 3.9, and brain stem 175 ± 7.1; (ng DA/g tissue) striatal 5682 ± 155 and limbic 1395 ± 48.3; (ng 5-HTP/g tissue) striatal 113 ± 6.9, limbic 175 ± 7.9, hemispheral 77 ± 4.9, and brain stem 234 ± 13.0; (ng 5-HT/g tissue) striatal 219 ± 10.9 and limbic 491 ± 15.7. Control levels for compound **12**: (ng DOPA/g tissue) striatal 1281 ± 54.5, limbic 440 ± 16.5, hemispheral 100 ± 4.9, and brain stem 207 ± 8.3; (ng DA/g tissue) striatal 6286 ± 292 and limbic 1409 ± 50; (ng 5-HTP/g tissue) striatal 103 ± 5.5, limbic 195 ± 7.2, hemispheral 79 ± 3.0, and brain stem 314 ± 14.8; (ng 5-HT/g tissue) striatal 212 ± 5.6 and limbic brain portions 700 ± 30. Statistics: one-way ANOVA followed by Dunnett's t test; (*) $p < 0.05$, (**) $p < 0.01$ vs control.

(30) Andén, N.-E.; Carlsson, A.; Häggendal, J. *Annu. Rev. Pharmacol.* **1969**, *9*, 119–134.
(31) Carlsson, A.; Davis, J. N.; Kehr, W.; Lindqvist, M.; Atack, C. V. *Naunyn Schmiedeberg's Arch. Pharmacol.* **1972**, *275*, 153–168.
(32) Jacobs, B. L. *Life Sci.* **1976**, *19*, 777–786.

foreleg treading, jerks, flat body posture, sniffing, and stereotyped foreleg and head movements. This behavior was not antagonized by pretreatment with the DA receptor antagonist haloperidol (5.3 μmol/kg ip) or with haloperidol plus the adrenoceptor antagonist prazosin (2.6 μmol/kg ip).

Compound (4a*S*,10a*S*)-**11** (50 or 53 μmol/kg) induced a slight locomotor activity combined with stereotyped movements with the forelegs and occasional jerks in reserpinized rats. This latter behavior, which resembles that induced by DA-receptor agonists like apomorphine, was not antagonized by pretreatment with haloperidol or with the DA D_1-receptor antagonist SCH 23390[33] (1.7 μmol/kg sc). Compound (4a*S*,10a*S*)-**11** did not induce any biochemical changes in nonpretreated or in reserpine-pretreated rats. In contrast, (4a*R*,10a*R*)-**11** (50 or 53 μmol/kg sc) slightly decreased the DOPA levels in the striatal and limbic rat brain parts of nonpretreated rats. There was also a tendency toward elevated DA levels and diminished levels of homovanillic acid (HVA) after administration of (4a*R*,10a*R*)-**11**. Behaviorally, (4a*R*,10a*R*)-**11** induced a slight locomotor activity and occasional jerks. The enantiomers of the secondary amine **20** (63 and 50 μmol/kg sc) did not induce any significant biochemical or behavior effects except for a weak decrease of the DOPA level in the limbic system.

The biochemical and behavioral data presented above indicate that the enantiomers of **10** and **11** lack ability to directly stimulate 5-HT receptors. In addition, the behaviorally active **11** seems to lack DA-receptor stimulatory ability; the behavior induced by (±)-**11** was not counteracted by haloperidol or by SCH 23390. Thus, the pharmacological basis for the behavioral changes after racemic **11** or after any of the enantiomers is not understood.

The enantiomers of **12** markedly decreased the 5-HTP accumulation in all four brain regions of nonreserpinized rats at 0.32–3.2 μmol/kg sc and enhanced the concentration of 5-HT in the brain stem and hemispheres at 3.2 and 1.0 μmol/kg sc. These results are consistent with the potent serotonergic actions of the racemate.[10] The reduction in 5-HTP accumulation after (4a*S*,10b*S*)-**12** was more pronounced than after the same dose of (4a*R*,10b*R*)-**12**. The DOPA accumulation was increased in the brain stem and hemispheres after (4a*R*,10b*R*)-**12** (3.2 μmol/kg sc) and (4a*S*,10b*S*)-**12** (1.0 μmol/kg sc) were given. However, no changes in the DOPA levels were observed in the DA-rich areas (corpus striatum and limbic system) at these doses. The enantiomers of **12** (3.2 μmol/kg sc) induced a behavioral syndrome characterized by flat body posture and forepaw treading in resepine-pretreated rats (5-HT syndrome). Thus, (4a*R*,10b*R*)-**12** and (4a*S*,10b*S*)-**12** behave as potent 5-HT$_{1A}$-receptor agonists.

Affinity for 5-HT$_{1A}$-Binding Sites in Vitro. The enantiomers of **10–12** and a number of previously reported analogues (Figure 1) were evaluated for their direct effects on cortical 5-HT$_{1A}$-binding sites in the rat brain (Table IV). In general, the rank order of affinities from the binding studies agreed with the potencies determined in the in vivo studies; however, the binding studies were able to provide quantitative estimates of the affinity of low potency compounds for which accurate ED_{50} values could not be obtained in vivo and, thus, provided an additional basis for dividing the compounds into classes for the structure–activity analysis. As with the in vivo results, the binding studies demonstrated the very large enantiomeric differences shown by some of the compounds. For example, the enantiomers of **2** showed a greater than 1000-fold difference in affinities for the 5-HT$_{1A}$ site. In agreement with the in vivo data, two of the enantiomers of the octahydrobenzo[*g*]quinoline derivatives, (4a*R*,10a*S*)-**10** and (4a*S*,10a*S*)-**11**, showed extremely low affinity (K_i > 10 000 nM) for the 5-HT$_{1A}$ receptors. Another enantiomer in this series, (4a*R*,10a*R*)-**11**, also showed low affinity (K_i = 2807 nM), as expected from the in vivo work, but (4a*S*,10a*R*)-**10** had much higher affinity (K_i = 151 nM) than predicted by the in vivo results. The explanation of this apparent discrepancy is not known at present. One possibility is that the in vivo access of this enantiomer to the receptors or its metabolism is different than that of the other enantiomers. Another possibility relates to the fact that the in vivo assay was designed to test for agonist activity while the binding assay does not discriminate between agonists and antagonists; thus, it is possible that (4a*S*,10a*R*)-**10** may have primarily antagonist activity. The issue of the relative efficacies or intrinsic activities of the different enantiomers will require future study.

The affinities of the enantiomers of **12** for DA D_2 and α_1-adrenergic receptor sites were evaluated with [^{3}H]sulpiride[34] and [^{3}H]WB-4101[35] to label the respective sites.

Table IV. Affinity and Potency at 5-HT$_{1A}$ Receptors Defined by the Displacement of [^{3}H]-8-OH-DPAT and Approximate Biochemical ED_{50} Values

compound	K_i,[a] nM	slope[b]	N[c]	approx. ED_{50}[d]
(±)-**1**·HBr	3.18 ± 0.28	1.05 ± 0.03	6	0.06[e] (3b)
(2*R*)-**1**·HBr	4.11 ± 0.34	0.99 ± 0.12	3	0.1 (4b)
(2*S*)-**1**·HBr	6.11 ± 0.37	1.01 ± 0.07	3	0.2 (4b)
(±)-**2**·HCl	2.84 ± 0.25	1.09 ± 0.04	3	0.16[e] (4d)
(1*S*,2*R*)-**2**·HCl	2.08 ± 0.25	1.09 ± 0.07	4	0.06[e] (4d)
(1*R*,2*S*)-**2**·HCl	2920 ± 219	0.91 ± 0.04	4	>50[e] (4d)
(±)-**3**·HCl	104 ± 20	0.78 ± 0.08	3	
(2*S*,3*S*)-**3**·HBr	49.6 ± 4.2	0.87 ± 0.02	3	5 (4c)
(2*R*,3*R*)-**3**·HBr	1389 ± 31	1.04 ± 0.08	3	>43 (4c)
(±)-**4**·HCl	656 ± 7	1.01 ± 0.11	3	
(2*S*,3*R*)-**4**·HCl	2021 ± 302	0.97 ± 0.00	3	>50 (4c)
(2*R*,3*S*)-**4**·HCl	394 ± 38	0.88 ± 0.06	3	20 (4c)
(1*R*,2*S*)-**5**·HBr	8.04 ± 1.13	0.94 ± 0.12	3	0.3[e] (7)
(1*S*,2*R*)-**5**·HBr	923 ± 66	0.95 ± 0.04	3	40[e] (7)
(1*R*,2*S*)-**6**·HBr	16.9 ± 0.24	0.80 ± 0.07	3	0.3[e] (7)
(1*S*,2*R*)-**6**·HBr	501 ± 39	1.13 ± 0.05	3	>50[e] (7)
(±)-**7**·HCl	1037 ± 54	0.99 ± 0.05	6	>50[e] (4d)
(±)-**8**·HCl	1130 ± 187	0.96 ± 0.02	4	>50 (4e)
(±)-**9**·HCl	>10000[f]		3	>50 (4c)
(4a*R*,10a*S*)-**10**·HCl	>10000[f]		3	>50[g]
(4a*S*,10a*R*)-**10**·HCl	151 ± 18.2	0.97 ± 0.04	3	>50[g]
(4a*S*,10a*S*)-**11**·HCl	>10000[f]		3	>50[g]
(4a*R*,10a*R*)-**11**·HCl	2807 ± 497	0.96 ± 0.09	3	>50[g]
(4a*R*,10b*R*)-**12**·HCl	32.3 ± 3.2	0.85 ± 0.04	3	0.5[g]
(4a*S*,10b*S*)-**12**·HCl	3.87 ± 0.23	1.01 ± 0.21	3	0.5[g]

[a] K_i values are the apparent dissociation constants calculated using the Cheng–Prusoff equation (ref 48) and are given as the mean ± SEM. [b] Slope values were calculated by using nonlinear-regression analysis of the four parameter logistic equation described in Methods. [c] N = the number of separate experiments from which the mean and standard error were calculated. [d] Dose corresponding to a half-maximal decrease of 5-HTP formation in the limbic and striatal parts of rat brains. The appropriate references are given in parentheses. [e] In reserpine-pretreated animals. [f] Less than 50% inhibition of specific binding was seen at a concentration of 10^{-5} M of this compound. [g] Estimated from Table III, this paper.

(33) Christensen, A. V.; Arnt, J.; Hyttel, J.; Larsen, J.-J.; Svendsen, O. *Life Sci.* **1984**, *34*, 1529–1540.

The affinity of (4aS,10bS)-12 for D_2 sites (IC_{50} = 264 ± 54 nM) was around 20 times greater than that of (4aR,10bR)-12 (IC_{50} = 5530 ± 1810 nM). Both (4aS,10bS)- and (4aR,10bR)-12 had poor affinities for the α_1-receptor sites (IC_{50} values = 2427 ± 301 and 5170 ± 221, respectively). Similarly, the enantiomers of 11 were weakly potent in displacing [^{3}H]sulpiride from D_2-binding sites (IC_{50} values: (4aS,10aS)-11, 10035 ± 2714 nM; (4aR,10aR)-11, 4885 ± 817 nM). Interestingly, for 11 and 12 the enantiomer having the highest affinity for the 5-HT_{1A} receptor also had the highest affinity for the D_2 and α_1-receptors. Given that molecular biologic studies have shown that many of the G protein linked receptors have high structural homology, it might be imagined that the ligand recognition sites of these receptors have spatial and chemical similarities. Thus, it might not be surprising that the geometry of an enantiomer that makes it optimal for one G protein linked receptor would also make it the preferred structure of an enantiomeric pair for other G protein linked receptors as well.

Discussion

Pharmacology. The novel octahydrobenzo[g]quinolines 10 and 11 appeared to be inactive as 5-HT-receptor agonists in vivo but (4aS,10aR)-10 displayed a moderate affinity for 5-HT_{1A}-binding sites in vitro. Racemic (±)-11 induced a stereotyped behavior in reserpinized rats which was unaffected by treatment with D_1 or D_2 antagonists. Biochemical effects indicative of (weak) DA-receptor stimulation were observed after (4aR,10aR)-11 but not after (4aS,10aS)-11. Similarly, (4aR,10aR)-11 had a greater affinity for D_2-receptor sites than (4aS,10aS)-11, but the ability to induce stereotyped behavior resided in (4aS,10aS)-11. However, both enantiomers of 11 appeared to be weak DA D_2-receptor ligands.

The enantiomers of 12 showed a considerable affinity for 5-HT_{1A}-binding sites in vitro, the 4aS,10bS antipode being equipotent to 1 and 9-fold more potent than the enantiomer. Both enantiomers induced a behavior in reserpinized rats similar or identical in appearence with that observed after administration of 5-HTP. This was more pronounced after the 4aS,10bS enantiomer. Both enantiomers of 12 had poor affinities for α_1-sites. In contrast, (4aS,10bS)-12 had a moderate affinity for D_2 sites whereas the enantiomer was about 20-fold less potent in this respect. Thus, the selectivity of both enantiomers for 5-HT_{1A} receptors appears to be considerable.

Structure–Activity Relationships. Introduction of a methyl group in the nonaromatic ring of 1 or connection of one of the *N*-propyl substituents with C1 or C3 of the 2-aminotetralin moiety, thus forming the octahydrobenzo[g]- or [f]quinoline systems, results in several changes in conformational preferences and topography: (i) the amino group may be forced out of the plane of the aromatic ring as, for example, in 7 where the *N,N*-dipropylamino group prefers to adopt a pseudoaxial position,[36] (ii) a steric bulk is introduced which may be part of the 5-HT_{1A} receptor essential volume, and (iii) the mobility of the amino group may be restricted so that only one or sometimes two staggered rotamers are energetically accessible. As a consequence, such compounds have a more strictly defined direction of the N electron pair (N^+–H vector).[26] In addition, derivatives 1–4 and 7–13 represent a wide spectrum of serotonergic potencies and stereoselectivities (see Table IV). Therefore, this set of compounds constitutes a good basis for model development. To identify structural parameters which are important for activity, we followed the following protocol, which is closely related to the active-analogue approach.[37]

(i) Derivatives 5 and 6 were excluded from the set due to their conformational flexibility.[5]

(ii) The resulting set of compounds was divided into three subsets in accordance with the potencies of the compounds as 5-HT_{1A}-receptor agonists (Table IV): (a) potent agonists (K_i < 32.3 nM), (2R)-1, (2S)-1, (1S,2R)-2, (4aR,10bR)-12, and (4aS,10bS)-12; (b) agonists of moderate or weak potency (K_i = 49.6–394 nM), (2S,3S)-3 and (2R,3S)-4; and (c) compounds which lack agonist properties, "inactive" compounds (ED_{50} value > 43 mmol/kg), (1R,2S)-2, (2R,3R)-3, (2S,3R)-4, (±)-7, (±)-8, (±)-9, and the enantiomers of 10 and 11. We also included some additional, conformationally and pharmacologically well-characterized derivatives in the subsets: was added to group a, (4aR,10bS)-13[4f] and (2R)-5,6,7,8-tetrahydro-1-hydroxy-*N,N*-dipropyl-9*H*-benzocyclohepten-8-ylamine [(R)-28][4a] were added to group b, and (S)-28 and (4aS,10bR)-13, the inactive enantiomers, were added to group c.

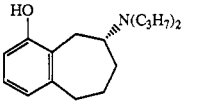

(2R)-28

(iii) A number of potential pharmacophore elements were identified: The hydroxyl group, the aromatic ring, the nitrogen, the nitrogen lone pair of electrons (N^+–H), and the vector formed by the nitrogen and its lone pair of electrons (the N^+–H bond). In addition, a dummy atom located 2.6 Å[40] from the nitrogen and aligned with the N^+–H bond vector was introduced in one of the models. This dummy atom was supposed to mimic a cation binding site (most likely, a carboxylate) at the receptor.

(iv) Hypothetical pharmacophore models consisting of two to four pharmacophore elements were generated. Each pharmacophore model was evaluated by fitting corresponding low-energy conformations of the potent agonists (subset a) as dictated by the model and then generating the combined van der Waals volume of the compounds. A pharmacophore model was rejected if it was unable to accommodate all derivatives in subset a. Similarly, the model was rejected if one of the inactive compounds in

(34) (a) *Sulpiride and Other Benzamides: Experimental and Clinical Pharmacology*; Spano, P. F., Trabucchi, M., Corsini, G. U., Gessa, G. L., Eds.; Italian Brain Research Foundation Press: Milan, Italy, 1979. (b) Spano, P. F.; Memo, M.; Govan, S.; Trabucchi, M. *Adv. Biochem. Psychopharmacol.* **1980**, *24*, 121–133.

(35) (a) Green, P. N.; Sharpero, M.; Wilson, C. *J. Med. Chem.* **1969**, *12*, 326–329. (b) U'Prichard, D. C.; Greenberg, D. A.; Snyder, S. H. *Mol. Pharmacol.* **1977**, *13*, 454–473.

(36) The conformational preferences of 7 have been studied by ^{1}H NMR spectroscopy and MMP2 calculations: ref 5.

(37) Marchall, G. R.; Barry, G. D.; Bosshard, H. E.; Dammkoehler, R. A.; Dunn, D. A. *ACS Symp. Ser.* **1979**, *112*, 205–226.

(38) *d*-LSD is a potent ligand for the 5-HT_{1A} receptor (ref 39).

(39) Hibert, M. F.; McDermott, I.; Middlemiss, D. N.; Mir, A. K.; Fozard, J. R. *J. Med. Chem.* **1989**, *24*, 31–37.

(40) According to MMX-calculations (ref 41), this particular distance represents an optimal electrostatic interaction which is reinforced by a hydrogen bond between a protonated nitrogen and a carboxylate ion.

(41) MMX is a molecular mechanics program that is an enhanced version of Allinger's MMP2 program. The MMX program is part of the molecular modeling package PCMODEL (Serena Software, P.O. Box 3076, Bloomington, IN 47402-3076).

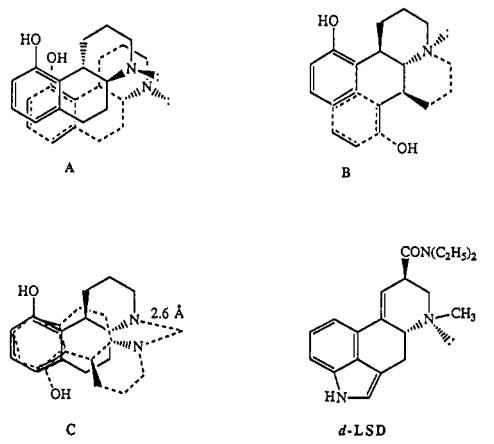

Figure 5. Three possible fitting modes, examplified by the enantiomers of **12**. *d*-LSD are shown for comparison.

subset c was able to adopt a geometry corresponding to a pharmacophore conformation with a relative steric energy less than 3 kcal/mol without producing excess volume. Finally, a model was rejected if it failed to describe differences in activity among subsets a–c.

Several pharmacophore models for serotonergic tetralin derivatives have been suggested previously.[5,39] These were considered but rejected on the basis of the present set of compounds; e.g., a model which consists of four pharmacophore elements corresponding to the phenolic oxygen, the aromatic ring, the nitrogen, and the nitrogen lone pair (N^+–*H*) could be rejected due to the inability to superimpose all four elements of both enantiomers of **12**. The enantiomers of **12** may be accommodated by a three-point model in which the nitrogen lone pairs have been omitted (model A, Figure 5). However, such a model may be rejected because it does not rationalize the stereoselectivity of **2** (Figure 6). Similarly, other pharmacophore models, such as B, in which *d*-LSD is used as a template (two aromatic sites, the nitrogen, and its lone pair are used as pharmacophore elements; Figure 5) could be rejected since the enantiomers of **11**, which are inactive as agonists, were able to fit the pharmacophore without producing excess volume.

The pharmacophore model of choice (C; Figure 5) for the present set of compounds consists of two pharmacophore elements—an aromatic site and a dummy atom–nitrogen vector (vide infra).[42] This model was constructed by use of subset a and is defined (Table V) by y, the distance (2.1–2.6 Å) from the dummy atom to the plane of the aromatic ring; x, the distance (5.2–5.7 Å) from the normal of the aromatic center to the dummy atom; α, the angle (−28° to 28°) between a vector connecting the N and the dummy atom and a vector bisecting the triangle formed by the corresponding vectors for the enantiomers of **12**; and β, the angle (−4° to 0.4°) between the aromatic plane and that described by the enantiomers of **12** (because of their "extreme" geometries, the enantiomers of **12** define the outer limits of these latter descriptors of the model). In this model, different faces of the molecules have to be aligned to produce an optimal fit (C; Figure 5). This brings, e.g., the hydroxyl groups of (2*S*)-**1** and (4a*S*,10a*S*)-**12** into a similar relative position as the electron-rich pyrrole ring of *d*-LSD (cf. ref 4i). The range of distances and angles defined by set a may correspond to limits for an optimal fit to this pharmacophore model for potent agonism. The combined van der Waals volumes of subset a, which define a receptor-excluded volume, are shown in Figure 7.

Low-energy conformations of moderately potent compounds should not be able to fulfill all the requirements of a model based on potent analogues. Thus, the low agonist potencies of the compounds in subset b should be due to an inability of low-energy conformations to fit optimally to the pharmacophore defined by subset a, and/or to production of excess volume(s) as compared to the partial receptor-excluded volume defined above. In fact, none of the minimum-energy conformations of the moderately potent 5-HT$_{1A}$-receptor agonists fits perfectly within the pharmacophore model, although, when the global minimum conformation of (2*R*,3*S*)-**4** is fitted to the model, only y deviates 0.1 Å from the ranges of distances and angles defined by subset a (Table V). The trans diastereomer (2*S*,3*S*)-**3**, on the other hand, fits better to the pharmacophore model in a conformation with a τ_N value of 150°, an angle that deviates 30° from that of the minimum-energy conformation (Table V).[43] Similarly, no

Table V. Distances and Angles Describing the Fit to the Pharmacophore Model of the Compounds Discussed[a]

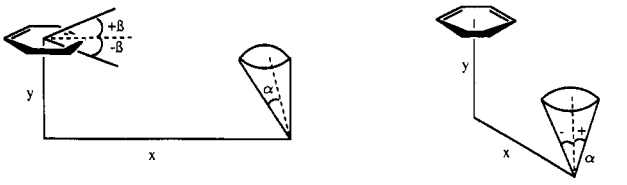

compd	y, Å	x, Å	α,[b] deg	β,[c] deg
d-LSD	2.6	5.2	−13	−4
(2*R*)-**1**	2.6	5.2	−9	0.4
(1*S*,2*R*)-**2**	2.1	5.7	−11	−3
(2*S*,3*S*)-**3**	1.0	6.9	−56	−13
(2*S*,2*S*)-**3**[d]	2.1	6.6	−30	−5
(2*S*,3*R*)-**4**	2.7	5.2	−16	0.4
(1*R*,2*S*)-**5**[e]	1.3	6.2	28	−8
(1*R*,2*S*)-**5**[f]	0.8	6.2	−1	−10
(1*R*,2*S*)-**5**[g]	0.1	6.3	−28	−15
(1*R*,2*R*)-**7**	2.5	1.7	58	−25
(1*R*,2*R*)-**7**[h]	1.0	6.2	51	−10
(1*R*,2*R*)-**7**[i]	1.7	6.5	28	−7
(2*R*)-**8**[j]	2.5	5.4	12	0.6
(2*R*)-**9**	0.4	5.8	72	−15
(2*R*)-**9**[k]	0.8	5.6	49	−9
(4a*R*,10a*S*)-**10**	1.0	7.0	−44	−10
(4a*S*,10a*S*)-**11**	2.7	5.2	−11	0.6
(4a*R*,10b*R*)-**12**	2.3	5.4	−28	0
(4a*R*,10b*S*)-**13**	1.9	5.8	49	−3
(2*R*)-**28**[l]	4.3	5.1	−28	13

[a] The global minimum energy conformation was used unless otherwise noted. [b] The other enantiomers have the opposite signs. [c] In relation to **12**. [d] A conformation derived from the minimum-energy conformation (ref 4c) by changing τ_N from 180°, to 150°. [e] Conformation a, ref 45. [f] A conformation derived from the minimum energy conformation (ref 45) by changing τ(C2′,C1′,C1,C2) from 58° to 90°. [g] A conformation derived from the minimum-energy conformation (ref 45) by changing τ(C2′,C1′,C1,C2) from 58° to 125°. [h] Conformation A, ref 5. [i] A conformation derived from conformation A (ref 5) by changing τ_N from 46° to 76°. [j] A conformation with equatorial nitrogen substituent, corresponding to conformation C (ref 21) of the 5-hydroxy isomer, relative steric energy, 1.9 kcal/mol. [k] A conformation derived from the minimum energy conformation (ref 4c) by changing τ_n from −164° to −134°. [l] A conformation derived from conformation I (ref 4a) by changing τ_N from −179° to 174°.

(42) The nonphenolic 2-(propylamino)tetralin possesses fairly high affinity for the 5-HT$_{1A}$ receptor (ref 4j). In addition, (*R*)-2-(dipropylamino)tetralin has been characterized as a fairly potent 5-HT$_{1A}$-receptor agonist based on in vitro and in vivo biochemical and behavioral data: Yu, H.; Liu, Y.; Lewander, T.; Hacksell, U. Manuscript in preparation. Thus, it appears to be justified to exclude the phenolic hydroxyl group from the pharmacophore.

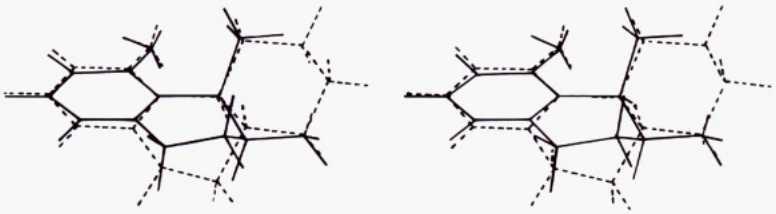

Figure 6. Computer generated (MIMIC) best fit of (1*R*,2*S*)-**2** (solid lines) and (4a*R*,10b*R*)-**12** (dashed lines). The nitrogen, the oxygen, and the midpoint of the aromatic rings were included in the fitting procedure. The average distance between fitted atoms was 0.03 Å. For clarity, the N-substituents have been omitted. The *cis*-1-methyl group of the inactive (1*R*,2*S*)-**2** occupies a similar relative position as the C1-methylene group of the potent (4a*R*,10b*R*)-**12**. Thus, the inactivity of the former compound could not be explained by this structural comparison.

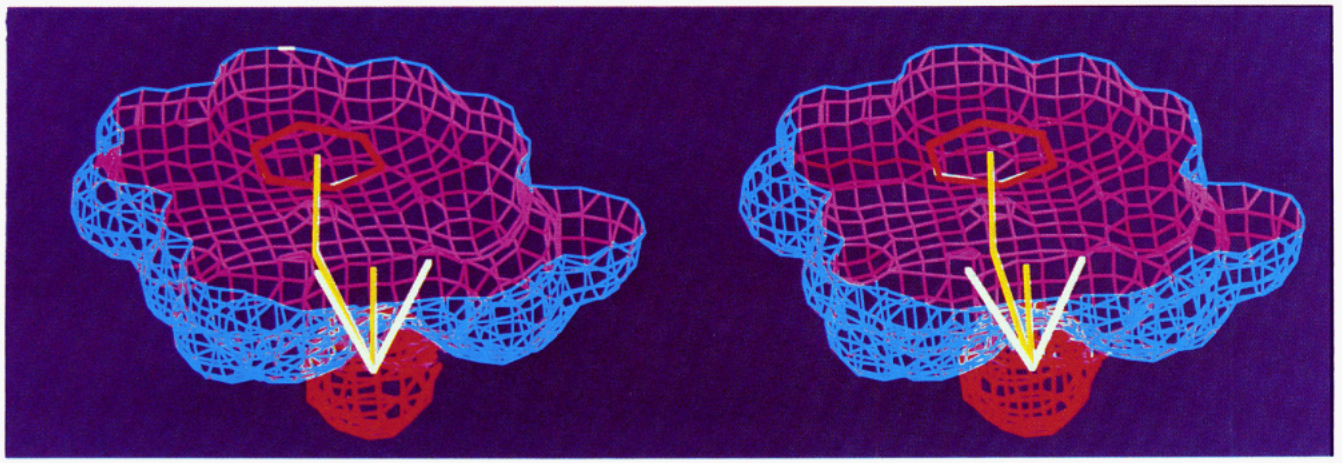

Figure 7. Combined van der Waals volume of the potent agonists (subset a). The 5-HT_{1A}-agonist pharmacophore model and the oxygen (red) with which the ammonium group is supposed to interact are included as reference points. The combined van der Waals volume has been sliced in a plane parallel to and 1 Å above the plane of the aromatic pharmacophore element (red). The white lines define the limit of the acceptable range of nitrogen–dummy atom vectors. The yellow lines correspond to descriptors defined in the text and in Table V.

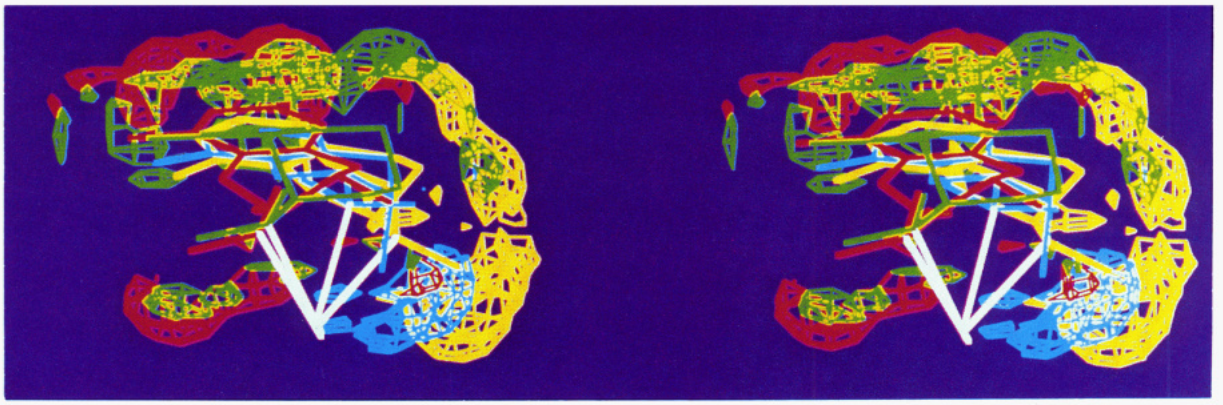

Figure 8. Excess volumes produced by the compounds in subset b, (2*S*,3*S*)-**3** (red), (2*R*,3*S*)-**4** (blue), (4a*R*,10b*S*)-**13** (yellow), and (2*R*)-**28** (green), compared to the volume defined by subset a. The structures of the compounds, with the hydrogens omitted and the nitrogen–dummy atom in white, are shown.

energetically acceptable conformation of (*R*)-**28** produces a perfect fit to the pharmacophore model. A conformation with $\tau_N = 174°$, derived from the minimum-energy conformation by a 7° rotation about the C–N bond, was chosen as the most likely candidate for a bioactive conformation of (*R*)-**28** since it gives a good α-value (−28°). The conformationally restrained (4a*R*,10b*S*)-**13** cannot adopt a conformation that fits within the pharmacophore model, but its minimum-energy conformation produces the best fit and was used in the modeling studies. Inclusion of the selected conformations of subset b into the model extends the pharmacophore: y = 1.9–4.3 Å, x = 5.2–6.6 Å, α = −30 to 49° and β = −5 to 13°. The excess volumes produced by these conformations are shown in Figure 8. It should be noted that the choice of bioactive conformations of the compounds in subset b is tentative and that they may not be optimally fitted to the pharmacophore model. In addition (vide supra), it is not known if the moderate potencies observed are due to the production of excess volume, a poor fit to the pharmacophore, and/or a considerable energy penalty.

Nevertheless, the extended model was useful when rationalizing the lack of agonist activity of the compounds in subset c. None of the energetically acceptable conformations of the inactive (2*R*)-**9**, (2*S*)-**9**, (4a*R*,10a*S*)-**10**,

(43) Such a conformation would be energetically accessible, cf. Figure 3 in Johansson, A. M.; Nilsson, J. L. G.; Karlén, A.; Hacksell, U.; Svensson, K.; Carlsson, A.; Kenne, L.; Sundell, S. *J. Med. Chem.* **1987**, *30*, 1135–1144.

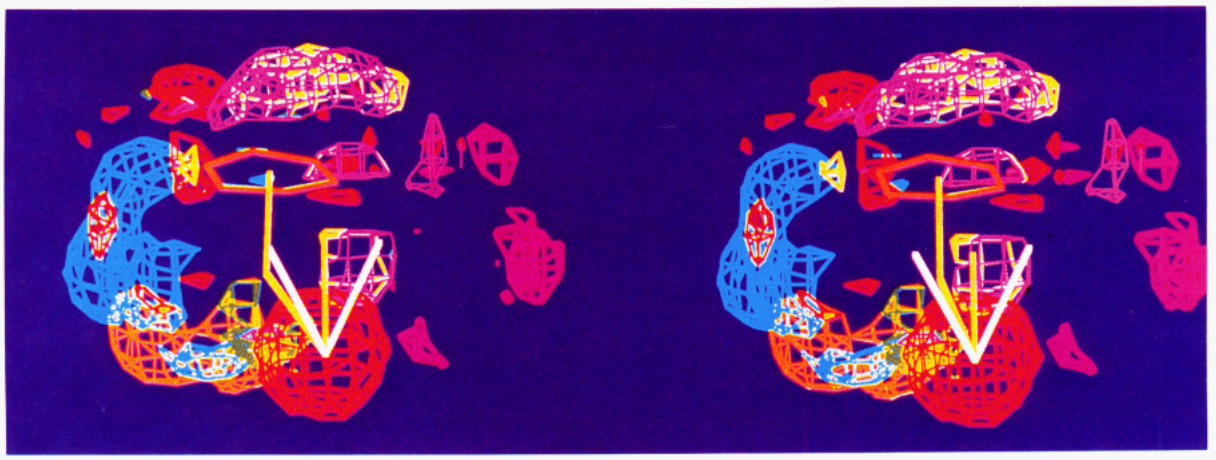

Figure 9. Excess volumes produced by some of the compounds in subset c, (1*R*,2*S*)-**2** (green), (2*R*,3*R*)-**4** (orange), (2*R*)-**8** (lilac), (2*S*)-**8** (yellow), (2a*S*,10a*S*)-**11** (blue), (4a*R*,10a*R*)-**11** (cerise), and (2*S*)-**28** (red), when compared to the combined volumes of subset a and b. The "pharmacophore model" which defines the aromatic center and plane, and the nitrogen–dummy atom vector orientations (the range of α-values) allowed for subset a, are shown. In addition, an oxygen atom with which the ammonium group of the ligands is supposed to interact is shown in red. Several of the inactive compounds produce excess volumes that overlap with this oxygen atom.

(4a*S*,10a*R*)-**10**, and (4a*S*,10b*R*)-**13** are able to fit within the extended pharmacophore model. However, some of the subset c analogues [(1*R*,2*S*)-**2**, (2*S*,3*R*)-**4**, the enantiomers of **11**, and (2*S*)-**28**] fit well to the extended pharmacophore model in low-energy conformations. Consequently, the inactivity of these latter derivatives appears to be related entirely to steric factors (Figure 9). Conformations of fairly high energy of (2*R*,3*R*)-**3**, (*R*)-**7**, (*S*)-**7**, and (±)-**8** fit to the extended pharmacophore model but produce excess volumes and it is, therefore, not possible to unambiguously identify one single factor which renders these compounds inactive. As none of the inactive derivatives but all of the agonists can be accommodated by the above 5-HT$_{1A}$-receptor agonist model, the model seems to be valid.

Several of the compounds in subset c [(1*R*,2*S*)-**2**, (2*S*,3*R*)-**4**, (1*R*,2*R*)-**7**, and (4a*R*,10a*R*)-**11**] produce excess volume in the proximity of the dummy atom (Figure 9). Such steric bulk may prevent a proper interaction between the protonated nitrogen and its anionic binding site and may constitute part of the 5-HT$_{1A}$-receptor essential volume.

Although the 1*S*,2*R* enantiomers of the phenylcyclopropylamines **5** and **6** possess a considerable conformational flexibility,[44] no conformation fits within the pharmacophore limits defined by subset a or b. As the minimum energy conformations of (1*S*,2*R*)-**5** and **6**, respectively,[45] only produce minor excess volumes compared to subset a when fitted to the pharmacophore model, they were considered as the most likely bioactive conformation (Figure 10a). However, in this and all other possible conformations the y value differs considerably from that of the pharmacophore model ($y < 1.0$ Å). Thus, if these compounds are included in the model the allowed range of y values has to be extended. Low-energy conformations of the inactive enantiomers of **5** and **6** which fit to this new extended pharmacophore model produce excess volume (Figure 10b). Similarly, excess volume is produced by other low-energy conformations; e.g., by a conformation of (1*R*,2*S*)-**5** which was constructed to produce the best α-value in relation to the model (Figure 10c). Part of this excess volume overlaps with the common excess volume produced by the enantiomers of **8** (Figure 9). It is noteworthy that models which include the active enantiomers of **5** and **6** do not accommodate subset b or c. Thus, the present model might be extended by inclusion of the active enantiomers of **5** and **6**.

Conclusions

The present study of conformationally restricted analogues of **1** led to the characterization of two new potent 5-HT$_{1A}$-receptor agonists, the enantiomers of **12**. These were instrumental in the development of a pharmacophore model which accommodates a rather large set of compounds with different stereoselectivities and agonist potencies and, thus, appears to have some generality. In fact, no outliers have been found so far. The model consists of a flexible pharmacophore and defines limits within which the relative position of an aromatic nucleus and a nitrogen–dummy atom vector may vary. It also defines a partial 5-HT$_{1A}$-receptor-excluded volume. The model does not take into account the electronic properties of the aromatic moiety. In addition, it does not define an optimal orientation of the *N*-alkyl groups. Still, this rather simple model may become a useful tool in the design of novel 5-HT$_{1A}$-receptor agonists.

Experimental Section

Chemistry. General Comments. Melting points (uncorrected) were determined in open glass capillaries on a Thomas-Hoover apparatus. Routine ^{1}H and ^{13}C NMR spectra were recorded at 90 and 22.5 MHz, respectively, on a JEOL FX 90Q spectrometer and were referenced to internal tetramethylsilane. ^{13}C NMR spectral data of some of the novel compounds are given in Table XIII of the supplementary material. IR spectra (recorded on a Perkin-Elmer 157 G spectrometer) and mass spectra (recorded at 70 eV, unless otherwise noted, on a 9000 LKB spectrometer using a direct-insertion probe) were all in accordance with the assigned structures. Optical rotations were obtained on a Perkin-Elmer 241 polarimeter. The elemental analyses (C, H,

(44) The rotation around the cyclopropyl–nitrogen bond appears to be restricted due to conjugation, cf.: Rall, M.; Harmony, M. H.; Cassada, D. A.; Staley, S. W. *J. Am. Chem. Soc.* **1986**, *108*, 6184–6189. Conjugation with the aromatic ring is also possible but the rotational barrier may be lower.

(45) The conformational preferences of **5** and **6** have been studied previously (ref 5) by MNDO calculations. In the present investigation, we have analyzed the conformational space available for **5** and **6** by use of molecular mechanics (MMX) calculations (ref 41). The latter calculations identified two additional low-energy conformations, conformation a (ΔE_S = 0 kcal/mol) and conformation b (ΔE_S = 0.1 kcal/mol) of (1*R*,2*S*)-**5**, having τ(C2′,C1′,C2,C1) = 58° and 145° and τ(C2,C1,N,N-electron pair) = 36° and 36°, respectively. The previously described low-energy conformation of **5** had a relative steric MMX energy of 0.1 kcal/mol.

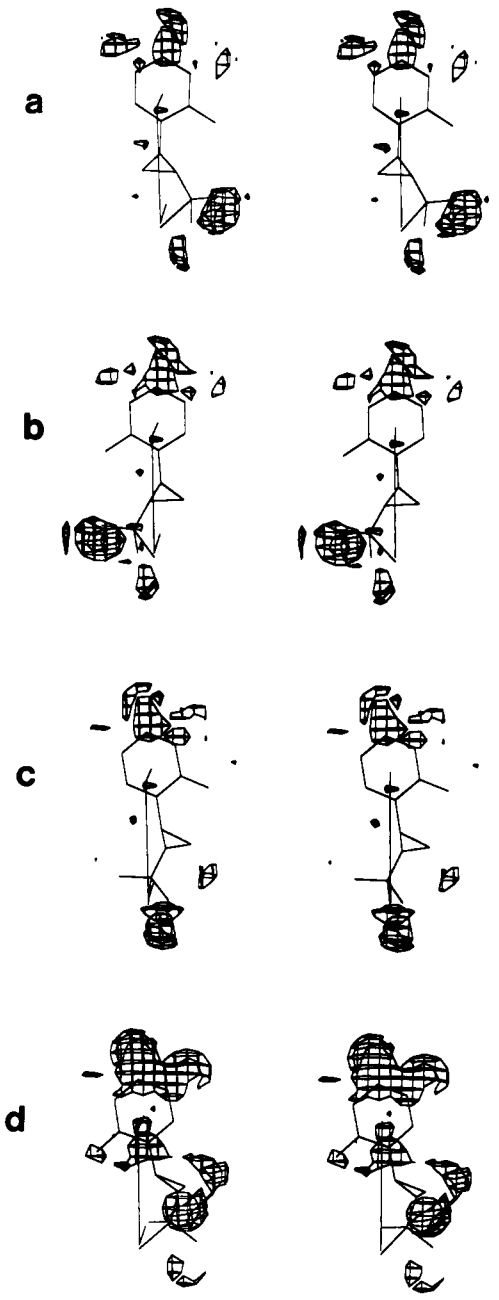

Figure 10. Excess volumes produced by (a) (1*S*,2*R*)-**5**, (b) (1*R*,2*S*)-**5**, (c) a higher energy conformation of (1*R*,2*S*)-**5** that fits to the model with the best possible α-value when compared to subset a, and (d) a conformation of (1*R*,2*S*)-**5** which adopts the same α-value as the "active conformation" of (1*S*,2*R*)-**5**. For conformational definitions, see the text.

and N), which were performed by Micro Kemi AB, Uppsala, Sweden, were within ±0.4% of the theoretical values except where noted. TLC was carried out on aluminum sheets precoated with silica gel 60 F_{254} (0.2 mm) and visualized with UV light and/or I_2. For the determinations of percent diastereomeric excess, capillary GC was performed on a Carlo-Erba 4200 instrument equipped with an SE 30 column (20 m, 0.32 mm) or a Carlo-Erba 6000 Vega instrument equipped with a DB-5 fused-silica column (30 m, 0.32 mm).

Synthesis. Below are given representative examples of the reactions presented in Table I.

Resolution of *cis*-1-Benzyl-1,2,3,4,4a,5,10,10a-octahydro-9-methoxybenzo[*g*]quinoline [(±)-(14)]. (−)-*O*,*O*′-Dibenzoyl-L-tartaric acid monohydrate (4.3 g, 11.4 mmol) was added to a hot solution of (±)-14[9] (3.5 g, 11.4 mmol) in EtOH (30 mL) and H_2O (10 mL). The solution was allowed to stand overnight at room temperature. The salt thus formed was recrystallized three times from EtOH/H_2O (3:1). The crystals were treated with 1 M aqueous NaOH and the free amine was extracted with ether. The organic layer was dried (K_2CO_3) and concentrated. The resulting solid was recrystallized from ether/light petroleum, yielding 1.2 g (69%) of (+)-(4a*S*,10a*R*)-**14**.

The free amine isolated from the mother liquors was treated with (+)-*O*,*O*′-dibenzoyl-D-tartaric acid monohydrate as described above. The precipitated salt was recrystallized twice from EtOH/H_2O. The free base was prepared and recrystallized to give 1.1 g (63%) of (−)-(4a*R*,10a*S*)-**14**.

The enantiomeric excess of (4a*R*,10a*S*)- and (4a*S*,10a*R*)-**14** was determined indirectly, as follows: The sample to be investigated [(4a*R*,10a*S*)- or (4a*S*,10a*R*)-**14**, 40 mg, 130 μmol] was converted into the hydrochloride by addition of ethereal hydrogen chloride to an ethereal solution of the amine. The ether was evaporated and the salt was dissolved in MeOH and hydrogenated over Pd(C). The catalyst was filtered off and the MeOH was evaporated. The resulting secondary amine was mixed with H_2O (0.20 mL) and 1 M aqueous NaOH (0.20 mL). A solution of (*R*)-2-methoxy-2-phenylacetyl chloride (193 mmol) [prepared from (*R*)-2-methoxy-2-phenylacetic acid (32 mg, 193 μmol) and thionyl chloride (2 mL), by stirring at room temperature for 2 h followed by evaporation of volatiles] in CH_2Cl_2 (0.5 mL) was added and the mixture was stirred vigorously at room temperature. The stirring was interrupted after 1 h and the organic layer was separated, washed with 1 M HCl, dried ($MgSO_4$), and concentrated. GC analysis of the crude amides indicated that the diastereomeric excess was >96% (column SE 30, flow 1 mL/min, 250 °C, t_R: (−)-enantiomer, 5.89 min; (+)-enantiomer, 5.97 min).

Resolution of *trans*-1-Benzyl-1,2,3,4,4a,5,10,10a-octahydro-9-methoxybenzo[*g*]quinoline [(±)-(18)]. (−)-*O*,*O*′-Di-*p*-toluoyl-L-tartaric acid (5.0 g, 13.0 mmol) was added to a hot solution of (±)-18[9] (4.0 g, 13.0 mmol) in 96% EtOH (50 mL). Ether (100 mL) was added and the solution was stirred overnight. The salt thus formed was recrystallized four times from EtOH. The free amine was liberated and precipitated from ether as the hydrochloride. One recrystallization from MeOH/ether afforded 1.3 g (58%) of (+)-(4a*S*,10a*S*)-**18**·HCl.

The other enantiomer, (−)-(4a*R*,10a*R*)-**18**, was obtained by fractional crystallization of the diastereomeric salts formed from the free amine recovered from the combined mother liquors and (+)-di-*p*-toluoyl-D-tartaric acid. After three recrystallizations, the amine was liberated and the hydrochloride was prepared and recrystallized to give 1.4 g (63%) of (−)-(4a*R*,10a*R*)-**18**·HCl.

The percent enantiomeric excess in (4a*R*,10a*R*)- and (4a*S*,10a*S*)-**18** was determined indirectly, by the same procedure as described above, to be greater than 96% (GC analysis, column SE 30, flow 1 mL/min, 250 °C, t_R: (−)-enantiomer, 6.66 min; (+)-enantiomer, 6.93 min).

(4a*S*,10a*R*)-1,2,3,4,4a,5,10,10a-Octahydro-9-methoxybenzo[*g*]quinoline Hydrochloride [(4a*S*,10a*R*)-15·HCl]. Method I. Ethereal HCl was added to a solution of (4a*S*,10a*R*)-**14** (1.0 g, 3.25 mmol) in ether. The precipitate was collected, dried and dissolved in MeOH (50 mL). Pd(C) (10%) was added and the mixture was hydrogenated at atmospheric pressure. The catalyst was removed by filtration (Celite), and the volatiles were evaporated. The residue was partitioned between ether and 1 M NaOH. The ether layer was dried (K_2CO_3), filtered, and concentrated. The secondary amine thus obtained was converted into the hydrochloride and recrystallized from MeOH/ether to give 0.63 g (76%) of pure (4a*S*,10a*R*)-**15**·HCl: ^{1}H NMR (CD_3OD) δ 7.24–7.05 (m, 1 H), 6.85–6.68 (m, 2 H), 3.82 (s, OMe), 3.90–3.68 (m, 1 H), 3.47–2.80 (m, 6 H), 2.50–2.18 (m, 1 H), 2.00–1.57 (m, 4 H); mass spectrum, *m*/*z* 217 (100, M^+), 134 (67).

***trans*-1,2,3,4,4a,5,10,10a-Octahydro-9-hydroxy-1-propylbenzo[*g*]quinoline Hydrochloride [(±)-11·HCl)]. Method II.** A solution of (±)-**21**·HCl (0.40 g, 1.4 mmol) in freshly distilled aqueous 48% HBr (10 mL) was stirred for 2 h at 120 °C under N_2. The volatiles were evaporated in vacuo and the solid residue was partitioned between ether and saturated aqueous $NaHCO_3$. The ether layer was dried (Na_2SO_4) and filtered. Ethereal HCl was added and the precipitate was recrystallized from MeOH/ether to afford 0.32 g (84%) of pure (±)-**11**·HCl: ^{1}H NMR (CD_3OD) δ 7.09–6.87 (m, 1 H), 6.70–6.49 (m, 2 H), 3.85–1.25 (m, 16 H), 1.07 (t, *J* = 7.2 Hz, 3 H); mass spectrum, *m*/*z* 245 (27, M^+), 216 (100, $M^+ - C_2H_5$).

***cis*-1,2,3,4,4a,5,10,10a-Octahydro-9-methoxy-1-propylbenzo[*g*]quinoline Hydrochloride [(±)-17·HCl]. Method III.** A solution of (±)-**15** (0.20 g, 0.92 mmol) and propionaldehyde (0.27 g, 4.6 mmol) in *n*-PrOH (4 mL) was hydrogenated over Pd(C) (10%) at atmospheric pressure. The catalyst was removed by filtration (Celite) and the filtrate was concentrated. The residue was eluted through a short alumina column with ether/light petroleum 1:4 as eluant. The purified amine was converted into the hydrochloride and recrystallized from MeOH/ether to afford 0.24 g (88%) of pure ±**17**·HCl: ^{1}H NMR (CD_3OD) δ 7.25–7.02 (m, 1 H), 6.86–6.63 (m, 2 H), 4.15–3.75 (m, 1 H), 3.84 (s, OMe), 3.50–2.75 (m, 8 H), 2.68–2.27 (m, 1 H), 2.11–1.37 (m, 6 H), 11.12–0.90 (t, J = 7.2 Hz, 3 H); mass spectrum, m/z 259 (33, M^+), 230 (100, $M^+ - C_2H_5$).

***trans*-4-Benzyl-1,2,3,4,4a,5,6,10b-octahydro-10-methoxybenzo[*f*]quinoline [(±)-23].** Trifluoroacetic acid (5 mL) was added dropwise to an ice-cooled mixture of (±)-**22**[10] (10.0 g, 44.2 mmol) and triethylsilane (15.1 g, 129 mmol) in CH_2Cl_2 (100 mL). The mixture was allowed to reach room temperature and was stirred for 65 h. The solution was concentrated in vacuo. The residue was dissolved in CH_2Cl_2 and was washed twice with 1 M aqueous NaOH. The organic layer was dried ($MgSO_4$), filtered, and concentrated. The solid residue was recrystallized from $CHCl_3$ and ether, yielding 8.14 g (80%) of an inseparable 1:4 mixture (according to capillary GC) of the trans and cis diastereomers.

A sample of the diastereomeric mixture (125 mg, 0.54 mmol) was dissolved in THF (25 mL) and the solution was slowly added to a slurry of $LiAlH_4$ (0.40 g, 10 mmol) in THF (75 mL). The mixture was heated to reflux for 20 h. It was then cooled and quenched with water (0.4 mL), 15% aqueous NaOH (0.4 mL), and water (1.2 mL). The mixture was refluxed for 1 h and filtered, and the filtrate was extracted with 1 M aqueous HCl. The aqueous layer was made alkaline with Na_2CO_3 and was extracted three times with ether. The combined ether fractions were dried (K_2CO_3), filtered, and concentrated to yield 105 mg of the crude secondary amine.

The amine was dissolved in acetonitrile (5 mL), and K_2CO_3 (190 mg, 1.4 mmol) and benzyl chloride (56 mg, 0.44 mmol) were added. The mixture was stirred under nitrogen at room temperature. More benzyl chloride (10 mg, 0.079 mmol) was added after 2 days, and after 3 days the mixture was filtered and concentrated. The residue was dissolved in ether, washed with 1 M aqueous NaOH, and then extracted twice with 0.5 M aqueous HCl. The combined aqueous fractions were made alkaline with Na_2CO_3 and extracted with ether. The organic layer was dried (K_2CO_3), filtered, and concentrated to yield 120 mg of a crude mixture of the diastereomeric benzylic amines. The diastereomers were separated on a silica column with ether/light petroleum 1:4 saturated with ammonia as eluant. The yield of the first-eluated cis diastereomer was 83 mg (55%); R_f = 0.47. The trans diastereomer (±)-**23** was obtained in subsequent fractions: yield 20 mg (13%); R_f = 0.25; mp 256–258 °C (lit.[10] mp 100–140 °C); ^{1}H NMR ($CDCl_3$) δ 7.32–6.98 (m, 6 H), 6.71–6.61 (m, 2 H), 4.05 (d, J = 13 Hz, 1 H), 3.77 (s, OMe), 3.44 (d, J = 13 Hz), 3.15–0.8 (m, 12 H); mass spectrum (12 eV), m/z 307 (100, M^+).

(4a*R*,10b*R*,α*R*)- and (4a*S*,10b*S*,α*R*)-1,2,3,4,4a,5,6,10b-Octahydro-10-methoxy-4-(α-methoxy-α-phenylacetyl)benzo[*f*]quinoline (25 and 26). Method IV. Compound (±)-**24** (0.37 g, 1.46 mmol) was mixed with CH_2Cl_2 (60 mL) and 1 M aqueous NaOH (60 mL). A solution of (*R*)-2-methoxy-2-phenylacetyl chloride (2.6 mmol) [prepared from (*R*)-2-methoxy-2-phenylacetic acid (0.30 g, 2.6 mmol) and thionyl chloride (10 mL), by stirring at room temperature for 2 hours followed by evaporation of volatiles] in CH_2Cl_2 (5 mL) was added and the mixture was stirred vigorously for 1.5 h. The stirring was interrupted, the organic layer was separated, and the aqueous layer was extracted twice with CH_2Cl_2. The combined organic layers were washed with saturated aqueous Na_2CO_3 and 0.5 M HCl, dried ($MgSO_4$), and concentrated, yielding 0.55 g of a crude diastereomeric mixture. The diastereomeric amides were separated on silica columns with ether/light petroleum (1:9) as eluant. Each of the purified amides showed a diastereomeric excess larger than 98.9% de according to capillary GC, (column DB 5, flow 1.5 mL/min, 250 °C, t_R: **26**, 14.0 min; **25**, 15.1 min).

Compound **25**: R_f = 0.44 (ether/light petroleum 1:9); ^{1}H NMR ($CDCl_3$) δ 7.60–7.30 (m, 5 H), 7.20–6.99 (m, 1 H), 6.72–6.55 (m, 2 H), 4.93 (s, 1 H), 3.74 (s, 3 H), 3.47 (s, 3 H), 3.20–0.90 (m, 12 H); mass spectrum, m/z 365 (38, M^+), 159 (89), 147 (100).

Compound **26**: R_f = 0.61 (ether/light petroleum 1:9); ^{1}H NMR ($CDCl_3$) δ 7.60–7.30 (m, 5 H), 7.20–6.99 (m, 1 H), 6.72–6.55 (m, 2 H), 5.00 (s, 1 H), 3.74 (s, 3 H), 3.52 (s, 3 H), 3.20–0.90 (m, 12 H); mass spectrum, m/z 365 (41, M^+), 159 (86), 147 (100).

(4a*R*,10b*R*)-1,2,3,4,4a,5,6,10b-Octahydro-10-methoxybenzo[*f*]quinoline Hydrochloride [(4a*R*,10b*R*)-22·HCl]. Method V. Compound **25** (0.19 g, 0.53 mmol) was dissolved in dry THF (2 mL) under N_2. The solution was cooled on an ice bath and a 1 M solution of lithium triethylborohydride (1.16 mL, 1.16 mmol) in THF was added druing 10 min. The solution was stirred at 0 °C for 15 h and then poured into ice-cooled 1 M HCl. The aqueous layer was washed twice with ether, made alkaline with 5 M aqueous NaOH, and extracted four times with ether. The combined organic layers were dried (K_2CO_3) and concentrated. The resulting amine was converted into the hydrochloride salt and recrystallized to afford 76 mg (66%) of pure (4a*R*,10b*R*)-**22**·HCl: ^{1}H NMR (CD_3OD) δ 7.13 (m, 1 H), 6.75 (m, 2 H), 3.80 (s, 3 H), 3.47–2.75 (m, 9 H), 2.23–1.10 (m, 3 H); mass spectrum (17 eV), m/z 217 (100, M^+), 32 (58).

The organic layers from the washing of the aqueous layer above were combined, dried ($MgSO_4$), and concentrated to afford crude racemic 2-methoxy-2-phenylethanol.

Molecular Mechanics Calculations. The structural modeling was performed by use of the interactive computer graphics program MIMIC (methods for interactive modeling in chemistry).[27] Calculations were performed on a MICROVAX II computer. Computational times ranged from 1 to 30 mins/minimization.

Molecular Graphics Studies. The SYBYL molecular modeling system, (SYBYL version 5.21, Tripos Associates, St. Louis, MO, 1989) was used for molecular fitting and volume manipulation. The *N*,*N*-dimethylamino derivatives of the compounds were used throughout and (4a*S*,10b*S*)-**12** was used as a template in the least-square fitting procedure—the two end points of a 2 Å long normal centered at the aromatic ring centeroid and the end point (the dummy atom) of a 2.6 Å long vector orginating from the nitrogen and oriented along the nitrogen lone pair of electrons were fitted with the corresponding structural elements of (4a*S*,10b*S*)-**12** using the FIT command of SYBYL. In the fitting procedure, each of the end points of the "aromatic normal" were given the weight 1 and the dummy atom the weight 2. Combined van der Waals volumes were obtained by use of the MVOLUME command of SYBYL.

Crystallography. Data Collection and Processing. Intensity data were obtained at room temperature on a Siemens STOE/AED2 diffractometer equipped with a graphite monochromator and using Cu Kα radiation (λ = 1.5418 Å, θ_{max} = 70°) and ω–2θ scan technique. Data reduction included corrections for background, Lorentz, polarization, and absorption effects, and the final stage of the refinements included also an isotropic extinction correction factor (SHELX[46]) for each structure. The absorption corrections were based upon ψ scans of selected reflections with χ near to 90° and different θ. The unit-cell parameters were refined against angular settings (Θ-values) of strong well-centered reflections [72 for (–)-**12**·HCl, 104 for (+)-**15**·HCl, and 60 for (+)-**18**·HCl], accurately measured on the diffractometer within the range 37° < 2θ < 83°.

Structure Determinations of (–)-12·HCl, (+)-15·HCl, and (+)-18·HCl. The structures were solved by direct methods (SHELXS[47]) and refined by full-matrix least-squares method (SHELXS[46]). The nonhydrogen atoms (with full site occupancy) were refined anisotropically in all cases, whereas the hydrogens were treated somewhat differently in these compounds. In the structure of (–)-**12**·HCl the hydroxylic H(10) (cf. Figure 2) was located from a difference Fourier calculation and was held riding on its mother atom O(10), during the following calculations, while all the other H atoms were given geometrically assumed positions which were recalculated after each cycle of the refinement.

(46) Sheldrick, G. M. *SHELX 76: Program for Crystal Structure Determination*; University of Cambridge: Cambridge, England, 1976.
(47) Sheldrick, G. M. *SHELXS 84: Program for Crystal Structure Solution*; University of Göttingen: Göttingen, FRG, 1984 (personal communication).

Table VI. Crystal Data and Selected Details of the Refinement Calculations for the Three Compounds Studied by X-ray Diffraction

compound	(−)-12·HCl	(+)-15·HCl	(+)-18·HCl
formula	$C_{16}H_{24}NOCl$	$C_{14}H_{20}NOCl$	$C_{22}H_{30}NO_2Cl$
formula weight	281.82	253.77	359.66
space group	$P2_1$	$P2_12_12_1$	$A2^a$
a, Å	8.2581 (3)	7.3072 (3)	10.5281 (4)
b, Å	8.9326 (4)	12.3990 (5)	7.2177 (3)
c, Å	10.3246 (4)	14.8308 (12)	25.6400 (22)
α, deg	90.0	90.0	90.0
β, deg	93.476 (4)	90.0	97.75 (1)
γ, deg	90.0	90.0	90.0
V_c, Å^3	762.69 (5)	1343.7 (2)	1930.5 (2)
Z	2	4	4
$D_{c,X\text{-ray}}$, g cm^{-3}	1.23	1.25	1.24
$\mu_{CuK\alpha}$, cm^{-1}	21.63	24.05	18.50
$N_{unique,\ nonzero}$	1608	1398	1544
$N_{used\ in\ the\ refinement}$ with the limit	1426 $F > 6\sigma(F)$	1358 $F > 2\sigma(F)$	1459 $F > 6\sigma(F)$
no. of variables	179	158	254
$R = \sum\|\Delta F\|/\sum\|F_o\|$	0.054	0.039	0.046
$R_W = [\sum w\|\Delta F\|^2/\sum w\|F_o\|^2]^{1/2}$	0.077	0.065	0.070
weighting: g, in *SHELX*[b]	0.000062	0.00159	0.00015

[a] *A*2 is the same space group as *C*2 but with a different choice of unit cell. [b] Weight of the structure factors are estimated in SHELX as $w = \text{const}/(\sigma^2(F) + gF^2)$.

Nevertheless, all hydrogen positions in the structures of (+)-15·HCl and (+)-18·HCl were derived from electron-density maps and were held riding on their mother atoms during the subsequent calculations.

The X-ray analysis of (+)-18·HCl revealed the presence of some amount of disordered crystal water. Three major disorder sites, one of which is a special position (0,y,0), were realized for the water oxygen atom. According to the refined site occupancy factors the unit cell seems to contain totally about 3.5 H_2O molecules. The O(W) disorder sites were refined isotropically and no hydrogens were located for them.

Final R values together with crystal data and selected details of the refinement calculations are listed in Table VI. The list of observed and calculated structure factors is available directly from I.C. on request.

Pharmacology. Materials and Methods. Male Sprague–Dawley rats (Alab, Stockholm) weighing 170–230 g were used. Reserpine and haloperidol were dissolved in a minimal quantity of glacial acetic acid and made up to volume with 5.5% glucose solution. The other substances were dissolved in 0.9% NaCl plus a few drops of 2 M HCl and moderate heating when required. Throughout, injection volumes were 5 mL/kg.

Biochemistry. Substances to be tested were given as the hydrochlorides, subcutaneously in the neck region, to reserpine-pretreated (5 mg/kg, i.e., 9 μmol/kg sc, 6 h before) or non-pretreated rats. The aromatic L-amino acid decarboxylase inhibitor (3-hydroxybenzyl)hydrazine hydrochloride (NSD 1015; 100 mg/kg, i.e., 573 μmol/kg, ip or 60 mg/kg, ie, 287 μmol/kg sc) was given 30 min later.[31] After another 30 min the rat was killed by decapitation. The brain was removed and immediately dissected on an ice-cooled Petri dish into four parts: the corpus striatum, the limbic system, the rest of the hemispheres including the cerebellum, and the brain stem. The brain parts were kept in a freezer. The tissue was homogenized in 0.1 M perchloric acid containing glutathione, EDTA, and α-methyl-DOPA (internal standard). DOPA, DA, HVA, 5-HTP, and 5-HT were determined by means of HPLC (ion pair, reversed phase) with electrochemical detection.

5-HT_{1A}-Binding Assay. The measurement of 5-HT_{1A}-binding sites, with use of [^{3}H]-8-hydroxy-2-(di-*n*-propylamino)tetralin ([^{3}H]-8-OH-DPAT; New England Nuclear Corp., Boston, MA) was carried out essentially as previously described.[48] Rats (Sprague–Dawley, 150–250 g) were decapitated, the brains were rapidly removed and cooled in ice-cold saline, and the cortex dorsal to the rhinal sulcus was dissected. The tissue was homogenized in 40 volumes of ice-cold 50 mM Tris-HCl buffer (pH 7.4) and then centrifuged at 48000*g* for 10 min. The resulting membrane pellet was then washed four times by sequential resuspension in buffer and centrifugation. Between the second and third washes the resuspended membranes were incubated at 37 °C for 10 min to facilitate the removal of endogenous 5-HT. After the last wash the membranes were resuspended to a final concentration of 10 mg of tissue original wet weight/mL of buffer for use in the binding assays. Each assay contained the following: 1 mL of membrane suspension, 0.1 mL of drug dilution (or appropriate vehicle if no competing drug was added, and 0.9 mL of solution containing [^{3}H]-8-OH-DPAT, Tris, $CaCl_2$, and pargyline to achieve final assay concentrations of 1 nM, 50 mM, 3 mM, and 100 mM, respectively. The assays were incubated for 15 min at 37 °C, followed by vacuum filtration through Whatman GF/B filters. The filters were washed twice with 4 mL of ice-cold 50 mM phosphate buffer, dried, and counted by liquid scintillation spectrometry. Specific [^{3}H]-8-OH-DPAT binding was defined as the difference between binding in the absence and presence of 10 μM 5-HT. The inhibition of [^{3}H]-8-OH-DPAT binding by the various compounds was analyzed by nonlinear-regression analysis (PCNONLIN, Statistical Associates, Inc.) using the four parameter logistic equation described by De Lean et al[49] to obtain IC_{50} and slope values for the curves. IC_{50} values were converted to apparent K_i values by using the method described by Cheng and Prusoff.[50] [^{3}H]Sulpiride- and [^{3}H]WB-4101-displacement experiments were performed essentially as previously described.[51]

Acknowledgment. The financial support from the Swedish Board for Technical Development, the Swedish Medical Research Council (14X-502), the Swedish Natural Science Research Council, and the U.S. National Institutes of Health (Grants No. NS16605 and NS01009) is gratefully acknowledged. I.C. is indebted to professor P. Kierkegaard for his continuous support and encouragement. We thank Mrs. Georgina Lambert for skillful technical assistence, Dr. Urban Höglund for help with the statistics, Dr. Christer Sahlberg for GC analyses, and Dr. Anders Karlén for help with the molecular mechanics calculations.

Supplementary Material Available: Fractional atomic coordinates and equivalent isotropic temperature factors of the non-hydrogen atoms (Table VII), ring puckering parameters for the nonplanar six-membered rings (Table VIII), selected torsion angles (Table IX), intramolecular bond distances and bond angles involving the non-hydrogen atoms (Tables X and XI), bond lengths and bond angles in possible hydrogen bonds (Table XII), fractional atomic coordinates of the hydrogen atoms (Table XIII), bond distances and bond angles, involving the H atoms (Tables XIV and XV), anisotropic thermal parameters of the non-hydrogen atoms (Table XVI), and ^{13}C NMR spectral data (Table XVII) (30 pages). Ordering information is given on any current masthead page.

(48) Taylor, E. W.; Duckles, S. P.; Nelson, D. L. *J. Pharmacol. Exp. Ther.* **1986**, *236*, 118–125.
(49) DeLean, A.; Munson, P. J.; Rodbard, D. *Am. J. Physiol.* **1978**, *235*, E97–E102.
(50) Cheng, Y.; Prusoff, W. H. *Biochem. Pharmacol.* **1973**, *22*, 3099–3108.
(51) Nikam, S. S.; Martin, R. A.; Nelson, D. L. *J. Med. Chem.* **1988**, *31*, 1965–1968.